220
10-18

DR- 1949

MLM-1853

MLM-1853

MASTER

Metallographic Investigation of Two Large Radioisotopic Heat Source (LRHS) Capsules

J. E. Selle and K. L. Breakall

September 29, 1971

AEC Research and Development Report

MOUND LABORATORY
Miamisburg, Ohio
operated by

Monsanto

MONSANTO RESEARCH CORPORATION
a subsidiary of Monsanto Company
for the

U. S. ATOMIC ENERGY COMMISSION
U. S. Government Contract No. AT-33-1-GEN-53

DISCLAIMER

MLM-1853
TID-4500
UC-25

Metallographic Investigation of Two Large Radioisotopic Heat Source (LRHS) Capsules

J. E. Selle and K. L. Breakall

Issued: September 29, 1971

LEGAL NOTICE

PRINTED IN THE UNITED STATES OF AMERICA
Available from
National Technical Information Service
U. S. Department of Commerce
5285 Port Royal Road
Springfield, Virginia 22151
Price Printed Copy $3.00, Microfiche $0.95

MONSANTO RESEARCH CORPORATION
A Subsidiary of Monsanto Company

MOUND LABORATORY
Miamisburg, Ohio 45342

operated for

UNITED STATES ATOMIC ENERGY COMMISSION
U S Government Contract No AT-33-1-GEN-53

TABLE OF CONTENTS

TABLE OF CONTENTS (Continued)

ABSTRACT

Two unvented, 200-W Large Radioisotopic Heat Source (LRHS) capsules were removed from shelf tests in July 1970 for a complete metallographic analysis. One capsule was fueled with plasma-fired microspheres and the other capsule was fueled with a PuO_2 microsphere-molybdenum cermet. Examination of the capsules showed (1) 81.3% of the helium had been released by the fuel; (2) some swelling of the cermet fuel had taken place; and (3) the T-111 strength member of the microsphere fueled capsule was found to be cracked upon removal from the clad. Furthermore, the Ta-10%W liner in the microsphere fueled capsule had not only undergone considerable grain boundary oxidation but had also reacted with the impurities present in the fuel. The Ta-10%W liner and T-111 strength member from the Mo-cermet fueled capsule were not embrittled.

INTRODUCTION

In June and July 1969 two unvented, 200-W LRHS heat source capsules were loaded and subjected to shelf tests at the nominal operating surface temperature of 1100°C. One capsule was fueled with plasma-fired microspheres and the other capsule was fueled with a PuO_2 microsphere-molybdenum cermet produced in 1969 by the Battelle Memorial Institute. The capsule design and test configurations are given in Appendix C. Schematic diagrams of the configuration of each capsule along with necessary details are given in Figures C-1 and C-2. These capsules were arranged side by side in the test rig as shown in Figure C-3. Temperatures measured at various points in the setup ranged from 985 to 1120°C with most of them in the 1050 to 1120°C range. A chronological history of the tests is given in Table 1. The capsules were removed from test in July 1970 for a complete postmortem analysis. The purpose of the analysis was to first measure the amount of helium released by the fuel, to determine whether any swelling had taken place during the test, and to determine the extent of any fuel-liner reactions and other container interactions that may have taken place and to assess their effect on the integrity of the capsule.

Table 1

CHRONOLOGICAL HISTORY OF LRHS THERMAL SOAK TEST

Date	Time Elapsed (days)	Event
January 2, 1970	-	Tests started
January 4, 1970	2	Tests halted - temperature did not reach 1100°C; more shielding added
January 5, 1970	-	Tests restarted
January 13, 1970	8	Tests halted - furnace burned out
January 17, 1970	-	Tests restarted
January 24, 1970	7	Tests halted - electronics problems
February 5, 1970	-	Tests restarted
February 13, 1970	8	Tests halted - scheduled power shutdown
February 16, 1970	-	Tests restarted
July 27, 1970	161	Tests completed
	186 Total	

Each capsule will be discussed separately since the results of each analysis were appreciably different.

BMI CERMET CAPSULE

PROCEDURE

BMI Cermet Fueled Capsule Details of the annular fuel cermets are given in Appendix A. These data were supplied by Battelle Memorial Institute[1]. Dimensions of each cermet are listed in the order of insertion into the capsule at Mound Laboratory. The fuel rings were overcoated with two 0.0037 in. (average) CVD molybdenum coating followed by a 0.0033 in. (average) ThO_2 overcoat. Coating thicknesses on each annulus are also given in Appendix A.

Procedures and Observations on LRHS Capsule Dimensional measurements were made on the clad and are summarized in Table 2. These measurements suggest that some swelling of the clad occurred as a result of the gas between the clad and the strength member. After one end of the platinum clad was removed with a tubing cutter, the capsule slipped out of the clad easily.

Table 2

DIAMETER MEASUREMENTS ON LRHS CLAD

	Dome End (in.)	Center (in.)	Flare End (in.)
0°	1.739	1.756	1.718
120°	1.724	1.719	1.705
240°	1.731	1.738	1.709

The outside of the strength member appeared to be a uniform medium gray color, except for four dark spots along one side. This was probably the side on which the capsule rested during the test and therefore was in contact with the clad. Diametral measurements were made on the strength member and these are summarized in Table 3. The variations noted could be due, in part, to variations in the thickness of the alumina coating. Apparently little or no creep took place. Hardness measurements, taken with a portable hardness tester, gave values of R_c 30-37, which is equivalent to VHN 300-360. These are summarized in Table 4. Part of the surface near each hardness indentation was then filed off to expose shiny metal underneath and hardness measurements were again taken. These are summarized in Table 5. In general, the hardness after filing was only slightly less than the unfiled hardness. The hardnesses after filing ranged from R_c 28-36 which is equivalent to VHN 285-355. This suggests that the alumina coating may have contributed to the increase in hardness

of the strength member. In general, the strength member appeared to be ductile, and no difficulty was experienced during filing.

Table 3

DIAMETER MEASUREMENTS ON LRHS STRENGTH MEMBER

	Dome End (in.)	Center (in.)	Flare End (in.)
0°	1.611	1.614	1.614
120°	1.619	1.617	1.619
240°	1.615	1.615	1.613

Table 4

HARDNESS MEASUREMENTS ON LRHS STRENGTH MEMBER BEFORE FILING (ROCKWELL-C)

	Dome End	Center	Flare End
0°	32-33	30	30
120°	32-34	37	37
240°	35	34	37

Table 5

HARDNESS MEASUREMENTS ON LRHS STRENGTH MEMBER AFTER FILING (ROCKWELL-C)

	Dome End	Center	Flare End
0°	35	34	31
120°	28	34	36
240°	29	33	31

The capsule was then TIG welded into the drilling fixture which was fabricated from 2 in. copper tubing with copper end caps. Welding was done by hand in an argon-filled vacuum glovebox. During the time it took to evacuate the pass box, the capsule was contained in a water-cooled chill block. After the capsule was welded into the fixture a rubber gasket and flange were bolted over the drilling port to seal in the argon and to minimize oxygen absorption during subsequent transport operations. All transporting was done with the capsule immersed in water.

The fixture was then installed in the apparatus for helium release measurements, and the system was evacuated. Measurements were made to determine the volume of the system. While the fixture was installed in the apparatus it was confined to a pan of water to ensure that the

temperature of the capsule would be kept to a minimum. Drilling of the capsule was extremely difficult. Two carbide drills broke, and one high speed center drill wore away in drilling. Finally a third carbide drill was successful in penetrating the liner. The volume of gas released was so great that it exceeded the capacity of the system. The gas came out very slowly. Some was collected and found to contain 88.2% He, 9.4% Ar, 1.7% N_2, and 0.5% O_2.

Details of the helium release measurements are given in Appendix B. Calculations show that 81.3% of the theoretical helium was released from the capsule. In addition, 15.8% was released during high temperature heating to 2000°C.[2] Thus 97.1% of the theoretical helium was accounted for.

One end of the capsule was cut off with a rotary cutoff wheel using a silicon carbide wheel. After the end came off, the liner was rotated inside the strength member and was easily removed. Two lengthwise cuts and another circumferential cut were made on the liner to remove the fuel and shims. The fuel rings were intact but the water on the outside surface resulted in a soft coating or slurry on the outside. This slurry was apparently the ThO_2 coating on the fuel rings that soaked up moisture. The inside of the liner was shiny although alternating light and dark rings were observed. The light rings were adjacent to the fuel, while the dark rings were adjacent to the shims.

After the fuel was removed from the capsule, dimensional measurements on each annulus were made, and each cermet ring was inspected visually for any changes in appearance. Black, white, and green crystals were observed on some of the cermets, and samples were taken of various areas for x-ray powder diffraction analyses. Table 6 gives a summary of the results of these analyses. The presence of MoO_3 in the powder suggests that molybdenum in the fuel oxidizes within the capsule, and the oxide may be stabilized by the thoria or plutonia. The results of the dimensional measurements are summarized in Table 7. Some swelling of the fuel is indicated. More swelling may have occurred that was obliterated by the loss of the coating during removal from the capsule. Photomicrographs of the fuel after sectioning are shown in Figures 1, 2, and 3. Quantitative metallography of the spheres shown in Figure 3 indicate a stoichiometry of $PuO_{1.82\pm.05}$. This suggests a slight decrease in stoichiometry below that of the original starting material which was about $PuO_{1.88\pm.05}$.[3]

Regions of the capsule taken for metallography are shown schematically in Figure 4. An attempt was made to examine samples from the ends as well as the center and to examine all welds. The general procedure was to examine the polished samples in the unetched condition; make microhardness traverses as needed; and then examine the samples in the etched condition. This procedure avoided complication during microprobe analysis resulting from etching. Microhardness values are easier to obtain in the unetched condition because the grain boundary relief does not complicate the measurement. The various interfaces examined were: fuel-liner interface; liner-strength member; strength member-clad; outside of clad; fuel-shim interface. Each interface will be discussed separately.

Table 6

SUMMARY OF X-RAY DIFFRACTION ANALYSES

Description	Identification
Black crystals	ThO_2 major component MoO_3 minor component α-Al_2O_3 and tantalum lines present plus unidentifiable weak lines
White crystals	MoO_3 major component ThO_2 minor component α-Al_2O_3 lines present, plus some unidentifiable weak lines
Dark band of lines	Tantalum metal, α-Al_2O_3, ThO_2, possibly some PuO_2
Dark band	Tantalum metal, α-Al_2O_3, ThO_2, PuO_2
Green crystals	MoO_3
Rough side	ThO_2 major component Mo minor component
Next to liner	ThO_2 major component Mo minor component

Table 7

DIMENSIONAL DATA FOR BMI CERMET DISCS AFTER REMOVAL FROM CAPSULE

Specimen	Power (W)	Initial OD(in.)	Measured OD(in.)	Change (in.)	Initial Thickness (in.)	Measured Thickness (in.)	Change (in.)
AA65	24.49	1.364	1.364	0.000	0.407	0.411	+0.004
AA66	27.38	1.363	1.366	+0.003	0.450	0.449	-0.001
AA67	30.45	1.366	1.359	-0.007	0.490	0.498	+0.008
AA69	33.78	1.363	1.381	+0.018	0.553	0.559	+0.006
AA70	29.73	1.362	1.368	+0.006	0.538	0.534	-0.004
AA71	29.18	1.361	1.374	+0.013	0.505	0.498	-0.007
AA72	31.05	1.364	1.368	+0.004	0.510	0.514	+0.004

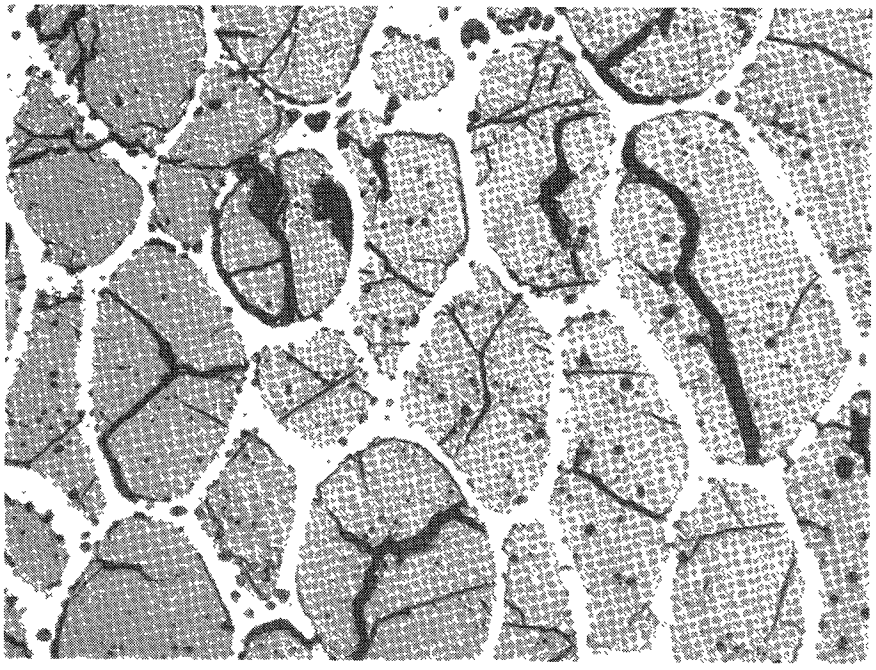

FIGURE 1 - Cross section of fuel disc taken from center of disc. (unetched, 250X)

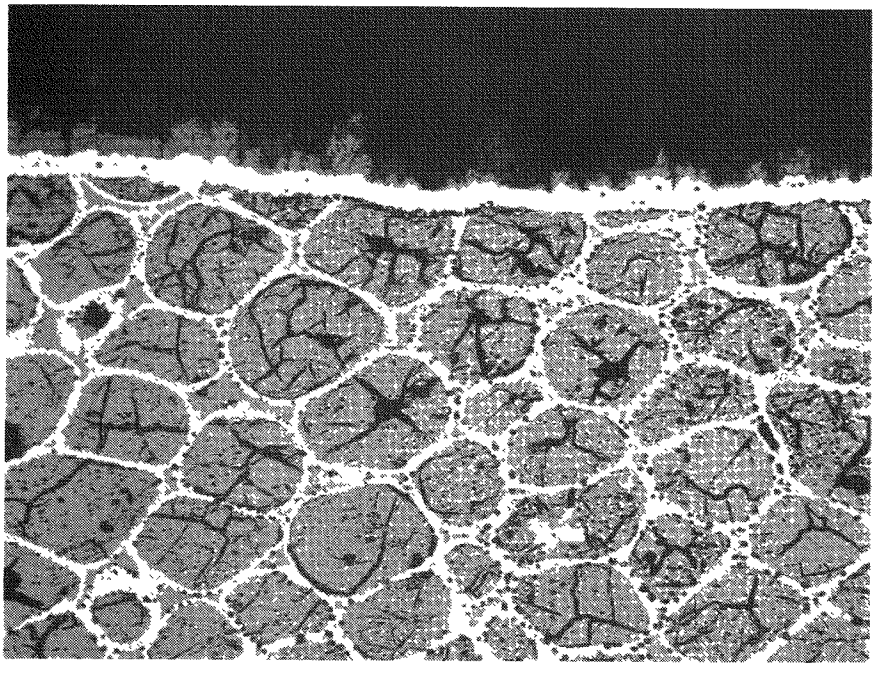

FIGURE 2 - Cross section of fuel disc taken from edge of sample showing molybdenum and ThO_2 overcoats. (unetched, 125X)

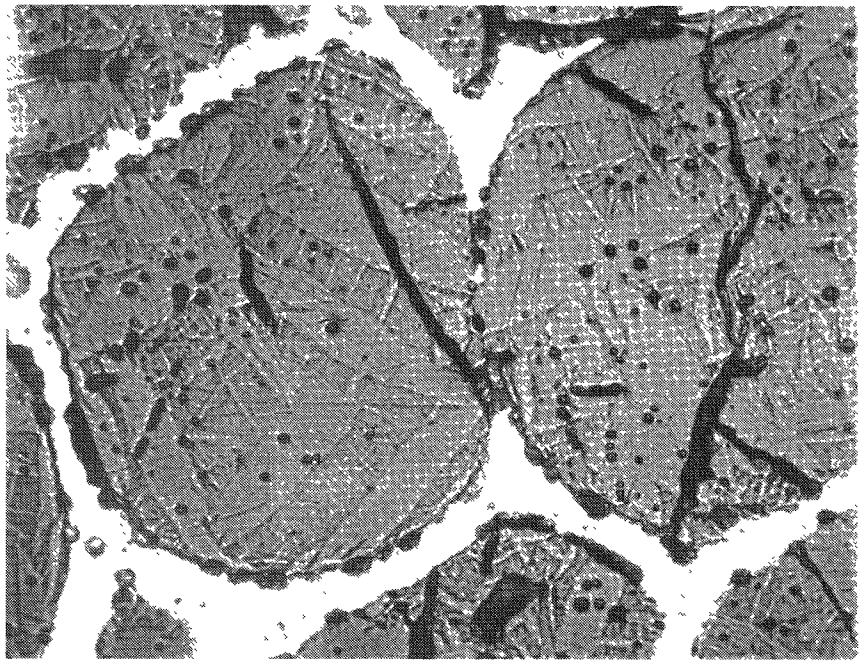

FIGURE 3 - Cross section of fuel disc showing area used for quantitative metallography. (unetched, 500X)

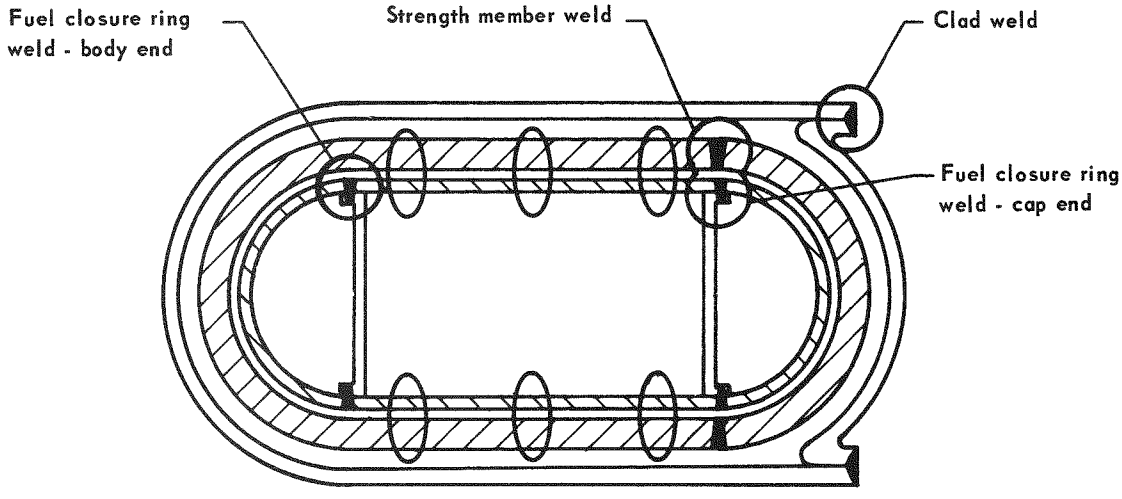

FIGURE 4 - Schematic of microsphere cermet capsule showing samples taken for metallography, including weld areas.

RESULTS AND DISCUSSION

Fuel-Liner Interface Two types of samples were obtained from the fuel-liner interface. Examination of the inside surface of the liner revealed alternating bands of light and dark material. The light bands were the same in appearance as the base metal. X-ray powder patterns made on scrapings from the dark band showed it to contain tantalum metal, α-Al_2O_3, ThO_2, and possibly some PuO_2. Also, a line was detected which could have been due to molybdenum. These data and relative thicknesses of the dark bands suggest that these bands were opposite the Ta-10%W spacers.

Metallographic analysis of the two regions showed appreciably different results. The dark area revealed the microstructure shown in Figure 5.

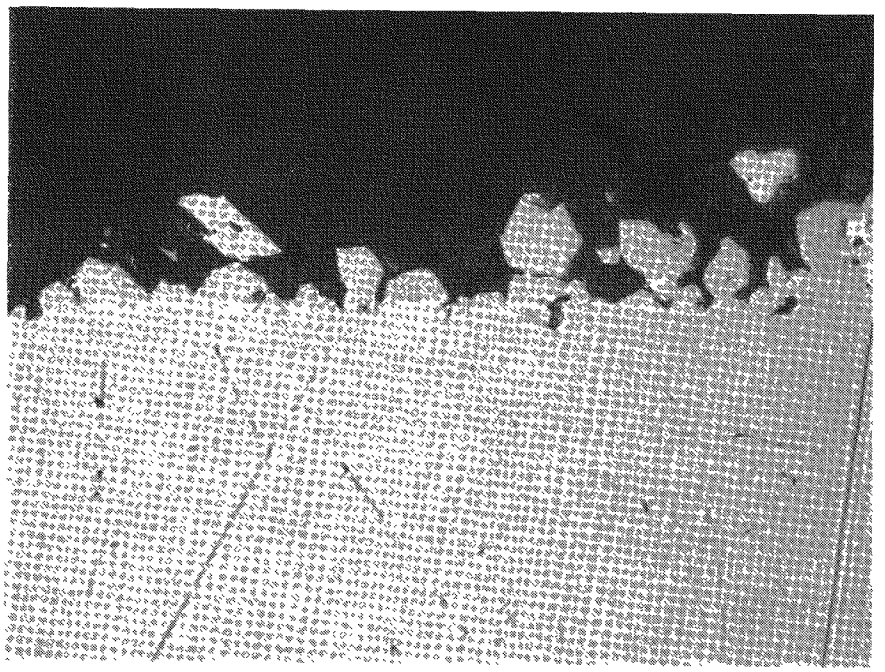

FIGURE 5 - Photomicrograph of the structure of the liner at the dark band opposite the shims. The microhardness traverse was made before etching the sample. (1240X)

The microstructure of the liner reveals nothing unusual except for a small deposit at the interface. A photomicrograph of the light area is shown in Figure 6. As seen in this figure, particles of tantalum oxide, Ta_2O_5, are seen dispersed rather evenly throughout the liner. Microhardness transverses made on each of these areas are shown in Figures 7 and 8. The hardness increase near the fuel-liner interface, Figure 8, indicates the diffusion of oxygen into the fuel to a depth of at least 14 mils. Between 14 and 20 mils the hardness is approximately background hardness, although peaks to a KHN level of 300 suggest at least some grain boundary diffusion of oxygen. The lower hardness values near the fuel-liner interface reflect the precipitation of Ta_2O_5 to a depth of 2-4 mils as suggested by Figure 6. In the dark areas the microhardness appears to increase from inside to outside. This is somewhat anomalous

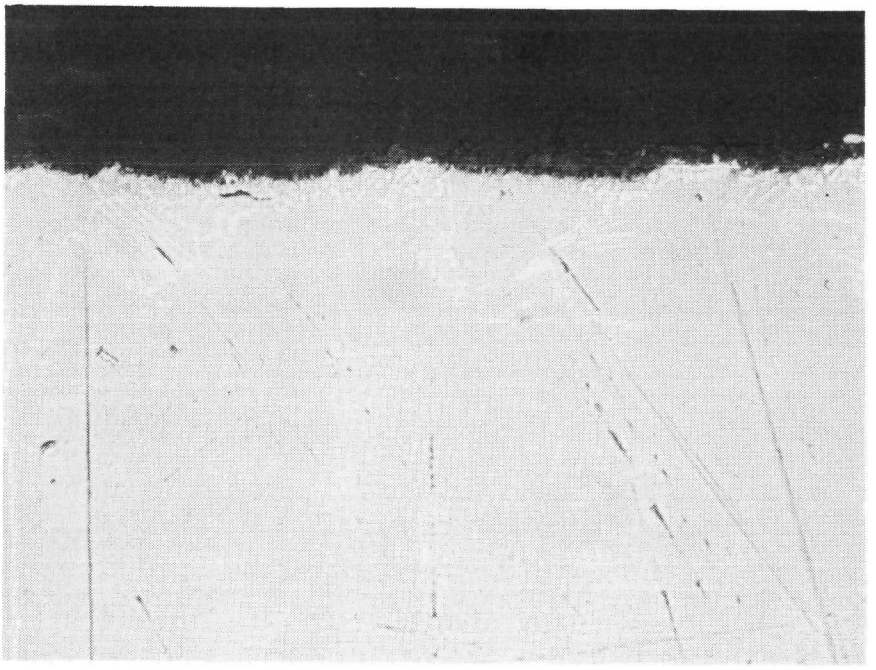

FIGURE 6 - Photomicrograph of the structure of the liner at the light band opposite the fuel rings. The microhardness traverse was made before etching the sample. (1240X)

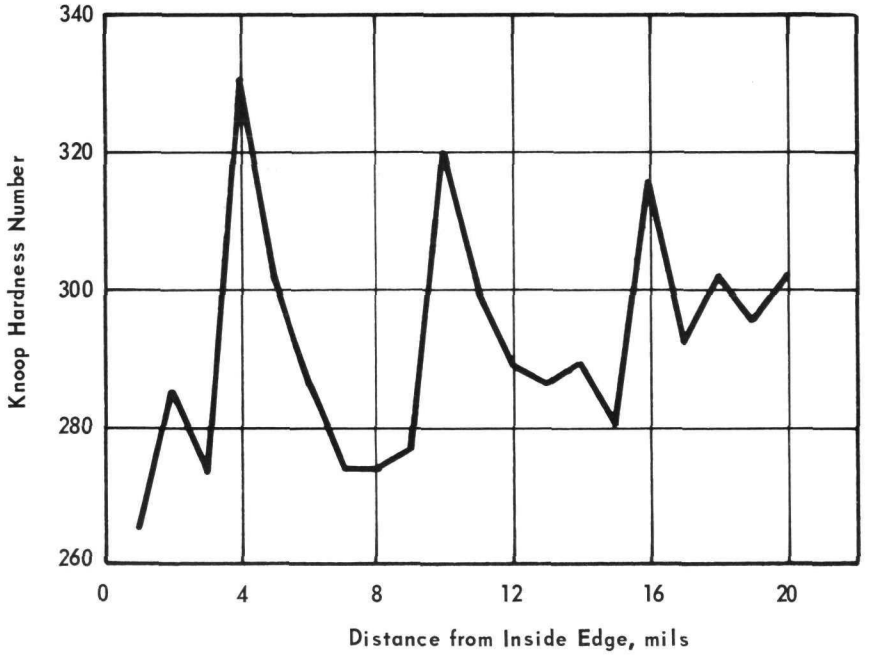

FIGURE 7 - Microhardness traverse across the liner at the dark band opposite the shims.

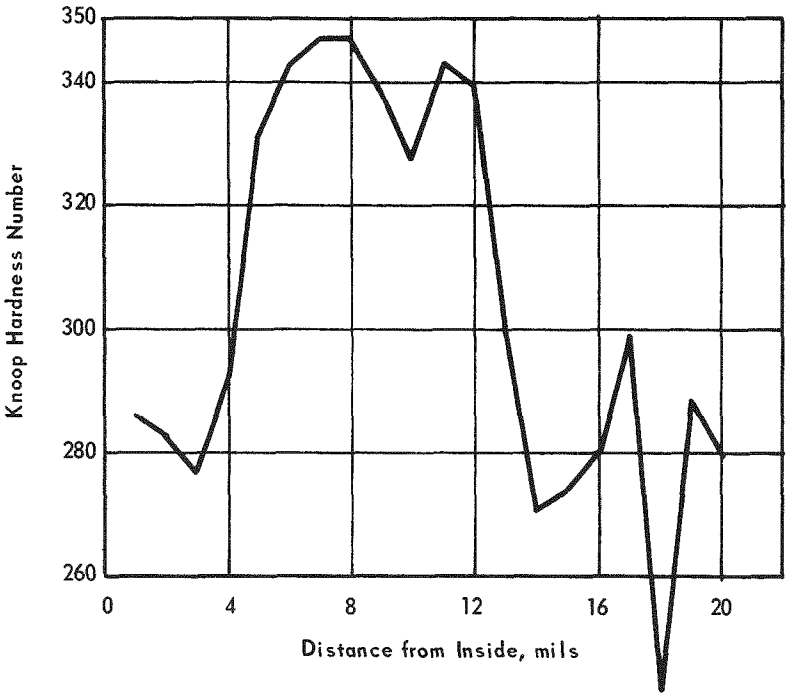

FIGURE 8 - Microhardness traverse across the liner at the dark band opposite the fuel rings.

and suggests that the sample may have oxidized during handling in the sectioning operation, although this could very well be due to scatter in the data.

Electron microprobe data on each area revealed that the reaction areas in Figure 5 resulted from the deposition or transfer of tantalum. Whether this resulted from vapor transfer or from contact is not known at this time. No tungsten or thorium was found in this region although there was a slight increase in the oxygen content in this deposit. In the light band area, adjacent to the fuel, no traces of plutonium thorium, or oxygen were found within the limits of sensitivity of the instrument.

Strength Member A photomicrograph of the strength member-clad interface is shown in Figure 9. The liner-strength member interface indicated no interaction. However, the strength member-clad interface shows a reaction band about 25 mils wide. Electron microprobe analysis revealed no interaction of any kind. Microhardness data, shown in Figure 10, show a considerable hardness increase in this region. While the data were recorded as Knoop Hardness Numbers, they have been converted to Vickers Hardness Numbers for this figure. This hardness increase is apparently caused by the interaction of the Al_2O_3 spray coating with the T-111. The point at which the hardness values leveled off can be correlated with the hardness indentations shown in Figure 9. A capsule that had been sprayed with Al_2O_3 but not subjected to high temperature was cross sectioned and examined for comparison. Microhardness data for this sample

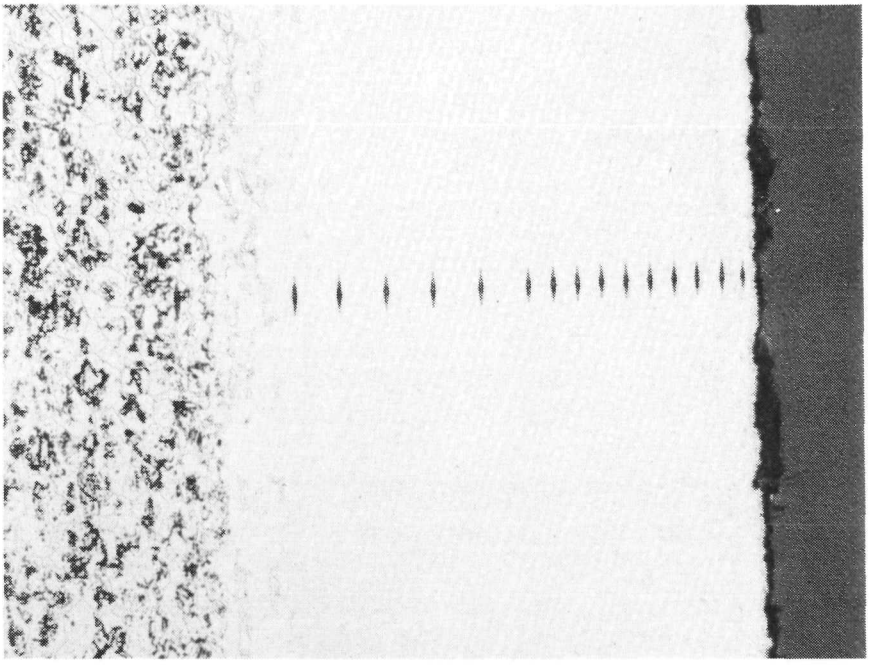

FIGURE 9 - Photomicrograph of the strength member at the outside edge showing a reaction layer about 0.025 in. wide. (125X)

are also given in Figure 10 and show only a slight increase in hardness near the sprayed interface. The hardness values obtained on the remainder of the strength member capsule appear to be essentially background values indicating little or no oxygen adsorption through the Ta-10%W into the T-111.

Electron microprobe analysis across the sample revealed a slight increase in aluminum near the alumina coating suggesting slight incompatibility between Al_2O_3 and T-111. This is also verified by the high microhardness values shown in Figure 10.

Clad A photomicrograph of the Pt-20%Rh clad is shown in Figure 11. The large grains indicate considerable grain growth during the test which would be expected. Also, some evidence of interaction between the alumina and the clad is indicated.

Spacers Since the spacers are adjacent to the fuel it is reasonable to expect some interaction between them. A photomicrograph of the interface (Figure 12) shows some evidence of a reaction in the form of Ta_2O_5 precipitates at the surface. Figure 13 shows microhardness traverses across a spacer. The inside edge was not adjacent to a fuel ring. The higher hardness values near the fuel interface is again an indication of oxygen absorption to a depth of about 5-10 mils from the interface.

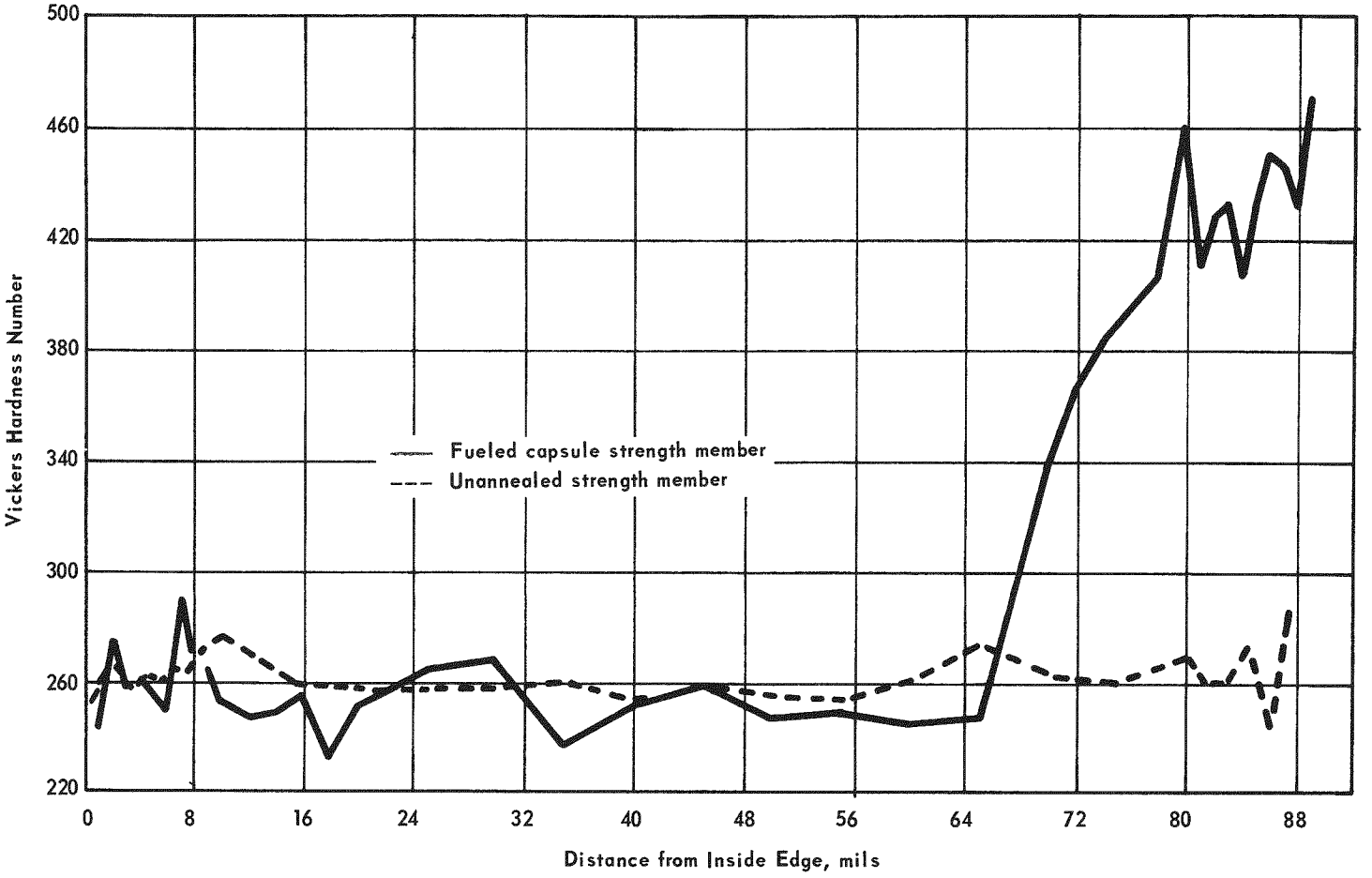

FIGURE 10 - Microhardness traverse across strength member.

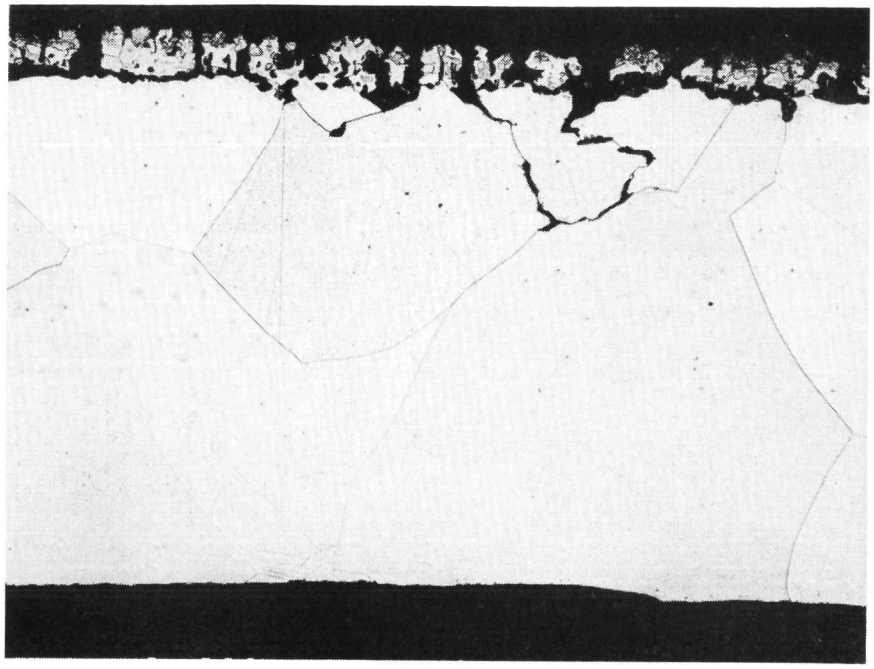

FIGURE 11 - Section of end cap of Pt-20%Rh clad of BMI fueled LRHS. (125X)

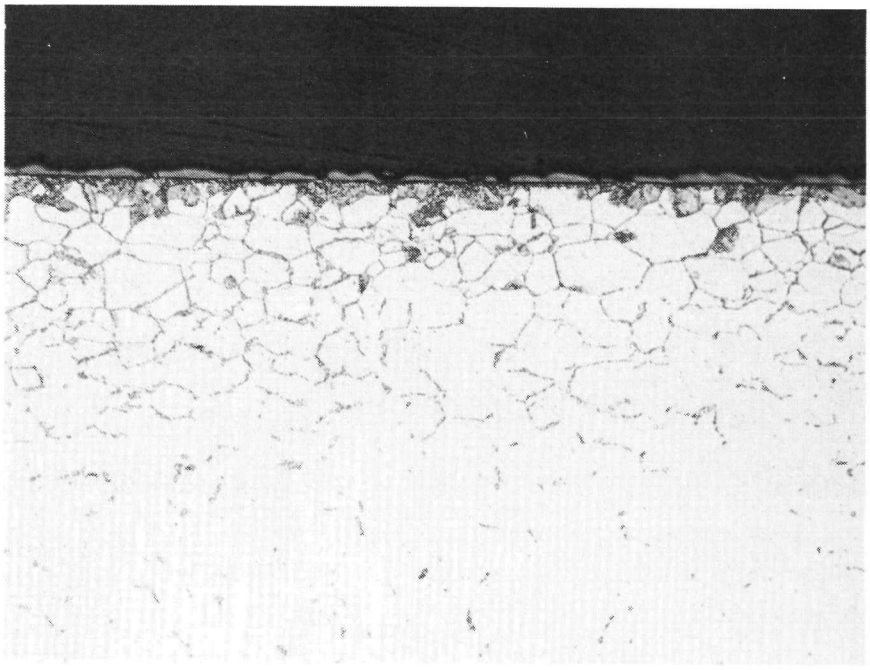

FIGURE 12 - Photomicrograph of spacer adjacent to a fuel ring. (250X)

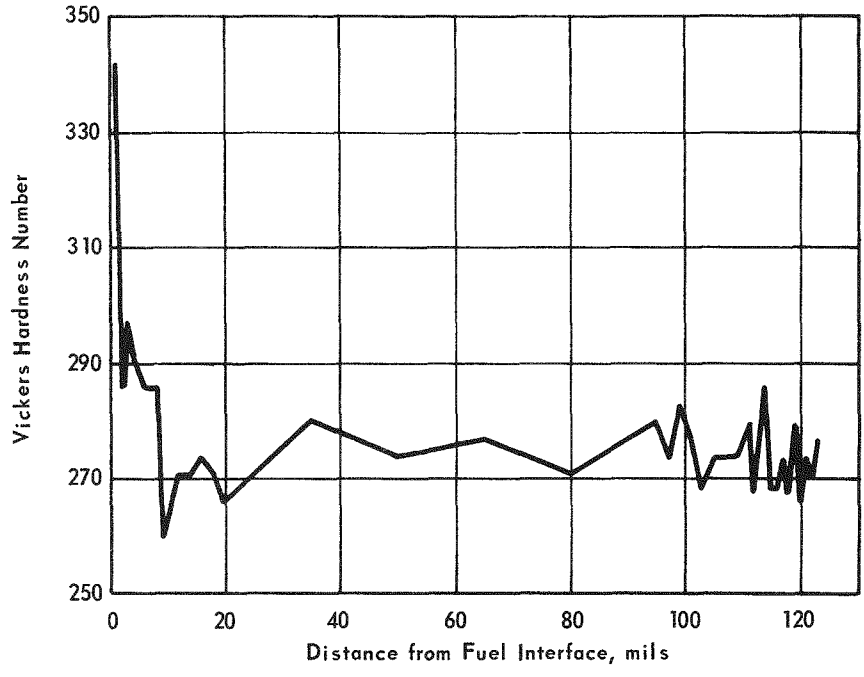

FIGURE 13 - Microhardness traverse across a fuel spacer.

Weld Analyses Photomicrographs of the various capsule welds are given Figures 14 through 17. It can be seen that the welds are sound and, with the exception of the strength member weld, had 100% penetration. The strength member weld showed 94% penetration.

Oxygen Analyses A summary of the oxygen content of samples taken from the BMI-fueled LRHS is given in Table 8. These values, particularly for the strength member, are considered low. The value of 1778 ppm for the strength member reflects the oxygen content of the Al_2O_3 spray coating on the outside. Samples of the liner and the strength member were bent with pliers 90° without cracking. Although the bend radius was much greater than 2T, this indicates some ductility at room temperature.

Table 8

SUMMARY OF OXYGEN ANALYSES OF SAMPLES TAKEN FROM THE CERMET FUELED LRHS

Sample	Oxygen Content (ppm)
Shims	33
Liner - dark band (shim area)	119
Liner - light band (fuel area)	174
Strength Member	1778
Strength Member (outer layer removed)	38

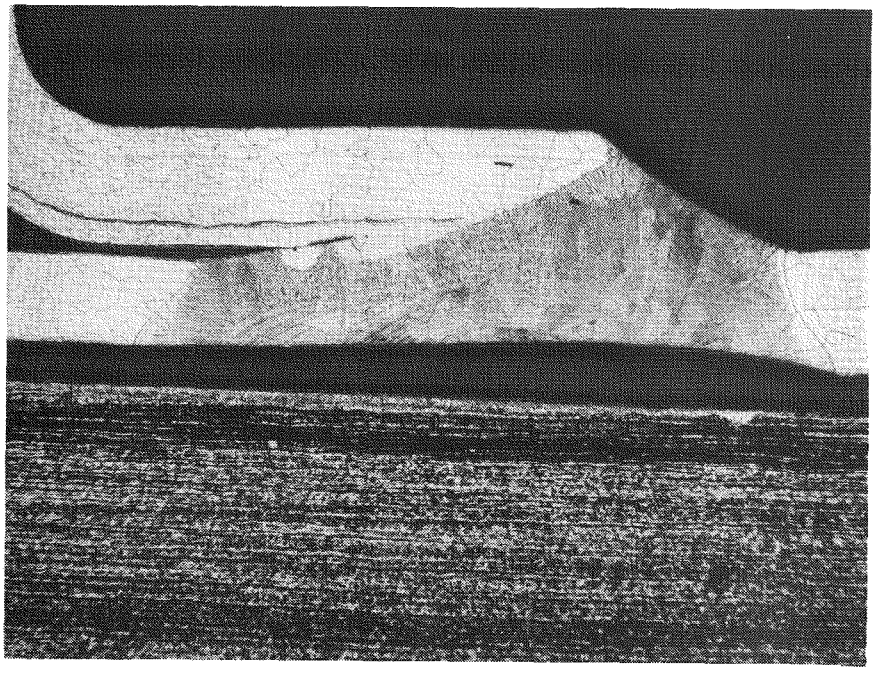

FIGURE 14 - Liner fuel closure ring weld, body end. (23X)

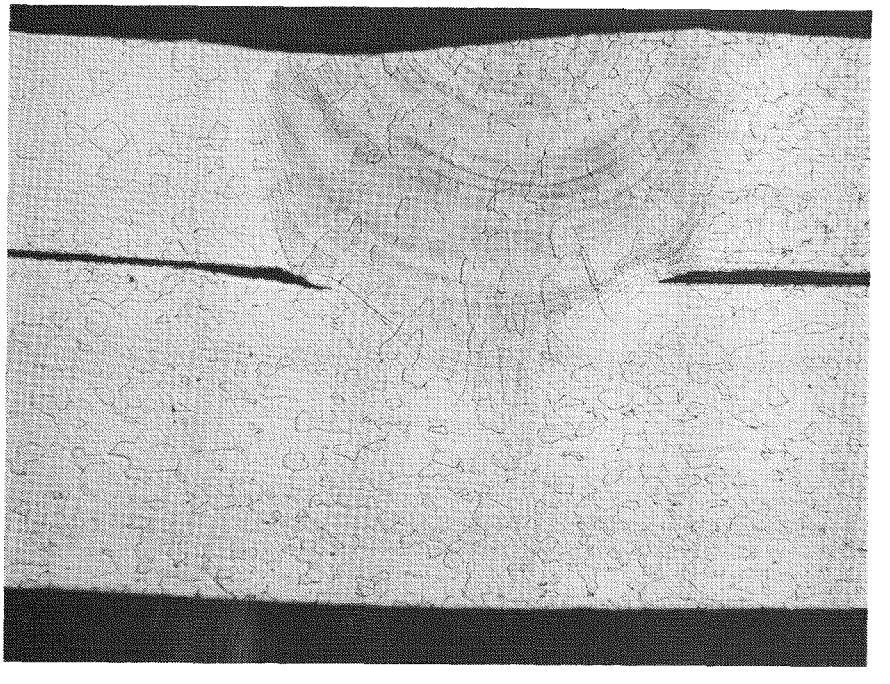

FIGURE 15 - Liner fuel closure ring weld, cap end. (72X)

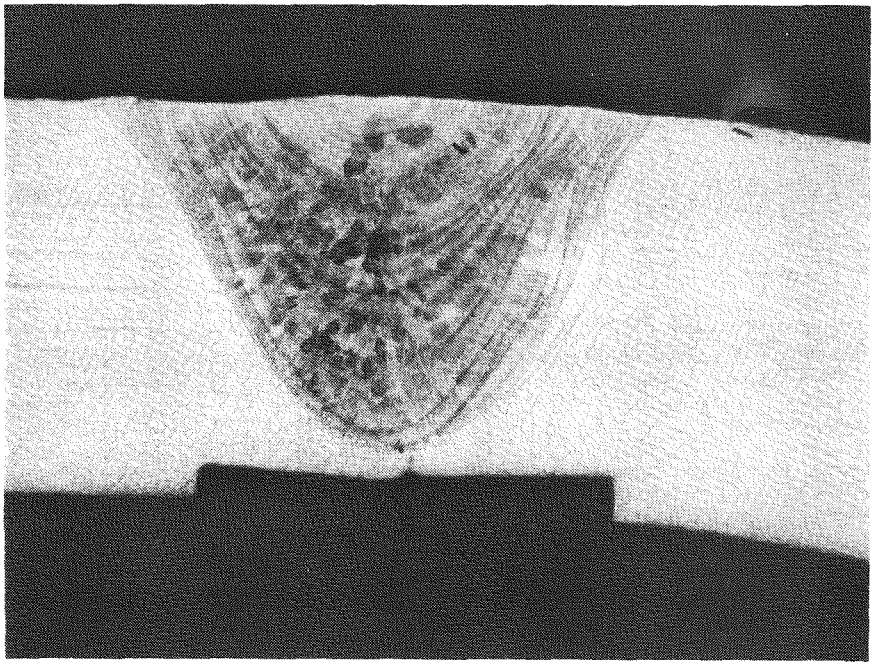

FIGURE 16 - Strength member weld. (23X)

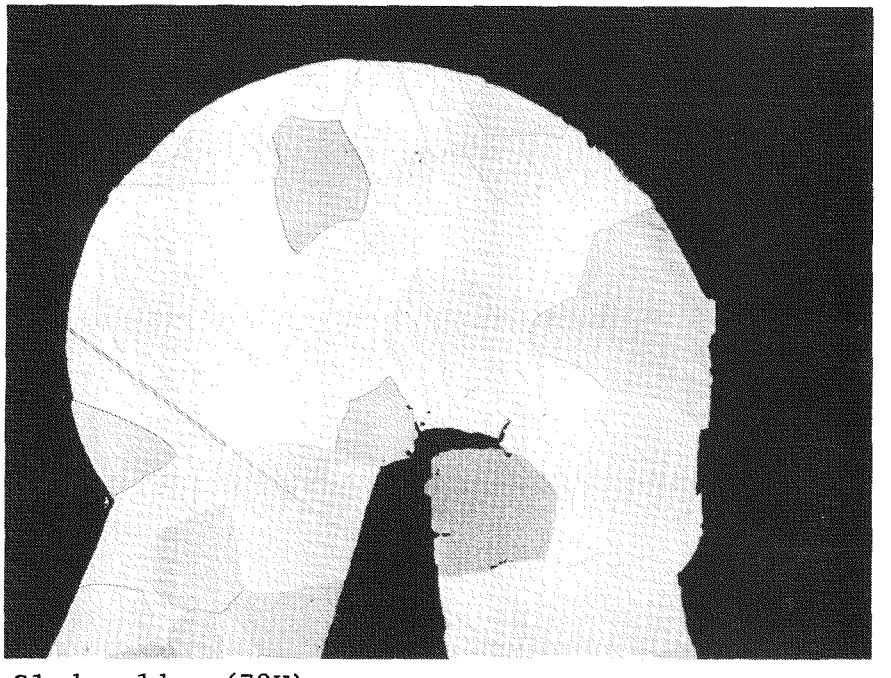

FIGURE 17 - Clad weld. (72X)

MICROSPHERE CAPSULE

PROCEDURE

Procedures and Observations on Microsphere LRHS Capsule Dimensional measurements made on the clad are summarized in Table 9. Some swelling occurred although the amount was less than in the cermet fueled capsule. The reason for this difference is not known. One end of the clad was removed with a tubing cutter. However, the capsule did not slip out as easily as did the cermet capsule. This was due, in part, to the deformation caused by the tubing cutter. When the capsule was removed from the clad, cracks were observed in the strength member and small gas bubbles were coming from these cracks. The capsule and the sink in the immediate area were contaminated. Photographs of the capsule surface, showing these cracks, are given in Figures 18 and 19.

Table 9

DIAMETER MEASUREMENTS ON MICROSPHERE-FUELED LRHS CLAD

	Dome End (in.)	Center (in.)	Flare End (in.)
0°	1.685	1.694	1.676
120°	1.677	1.698	1.687
240°	1.683	1.699	1.700

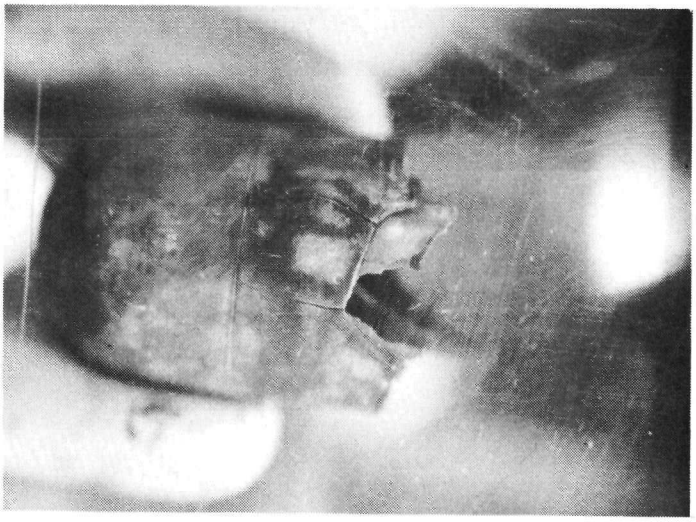

FIGURE 18 - Photograph of end of capsule showing a portion of the cracked surface.

Since the presence of these cracks negated the validity of any helium release measurements, the capsule was immediately transferred to the glovebox and cut open with a rotary cutoff wheel. A circumferential cut was made about 1-1/2 in. from one end of the capsule. This cut was made completely through the strength member and the outer liner. The inner liner resisted separation, and the capsule had to be broken with

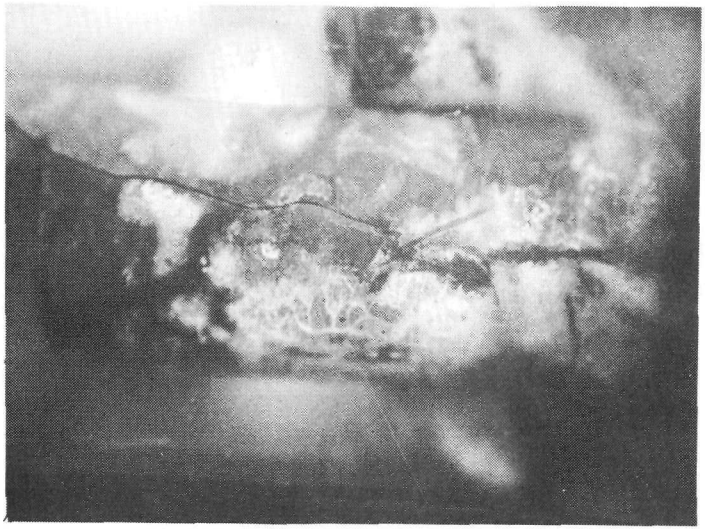

FIGURE 19 - Photograph of capsule showing lengthwise crack.

a blunt instrument to separate the two portions. Some of the fuel came out of the annular ring immediately, but most of it had sintered together and had to be scraped out with a sharp instrument. The capsule was quite hard.

Sections were taken for metallography as shown in the schematic diagram of Figure 20.

A cross section of microspheres taken from the capsule is shown in Figure 21. Five different artifacts can be seen in an apparently porous sample. These artifacts are identified in the photomicrograph and are explained as follows: the artifact labeled A is a void formed in the microsphere upon solidification, after passing through the plasma torch. Artifacts B are voids formed by the loss of individual grains during metallographic preparation. The small holes in spheres labeled C are the result of the phenomenon known as "plucking" which occurs curing metallographic preparation. Artifacts D are cracks, and artifacts E are grain boundary phases that usually contain iron and silicon. The presence of phase E seems to enhance the strength of an individual microsphere.

RESULTS AND DISCUSSION

Fuel-Inner Liner Interface A photomicrograph of the inner liner taken from the center of the capsule is shown in Figure 22. A higher magnification photomicrograph of the fuel-liner interface is shown in Figure 23. A reaction layer is seen at the interface and in the grain boundaries. Numerous grains fell out during the sectioning and polishing operations, and a number of intergranular cracks are seen. Electron microprobe analysis of the reaction layer at the interface revealed that the white layer contains high concentrations of iron and nickel which are impurities in the fuel. The small gray particles within this white layer contain plutonium. This impurity layer was not continuous as shown in Figure 24 which is a section taken from the short section of the inner liner.

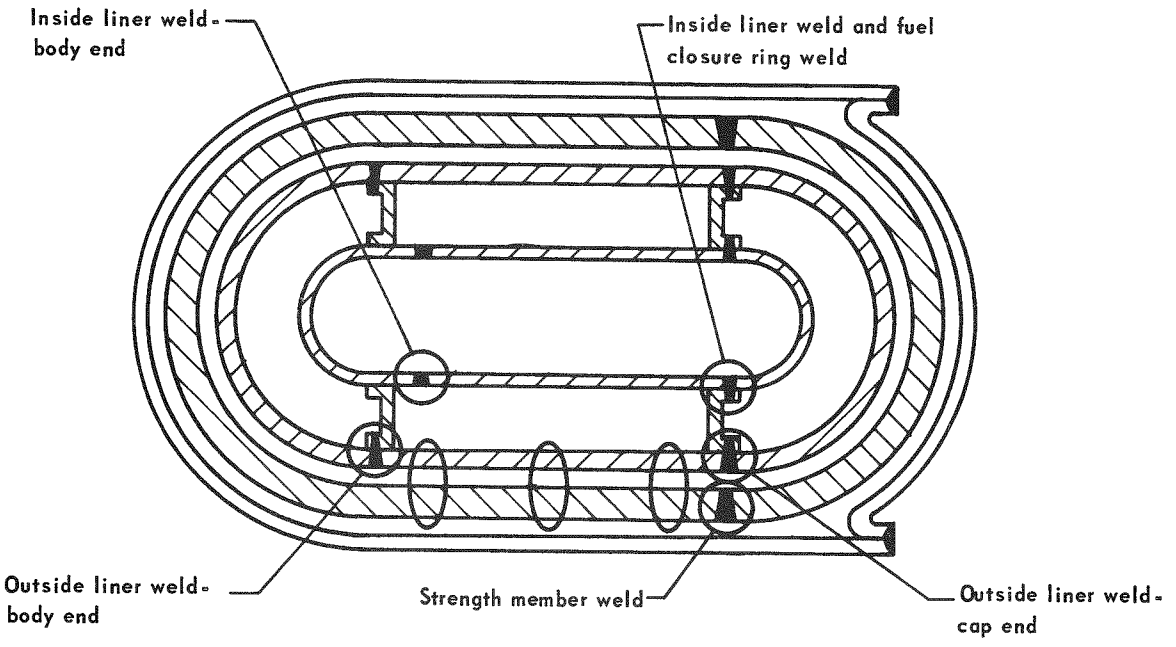

FIGURE 20 - Schematic of microsphere fueled capsule showing samples taken for metallography including weld areas.

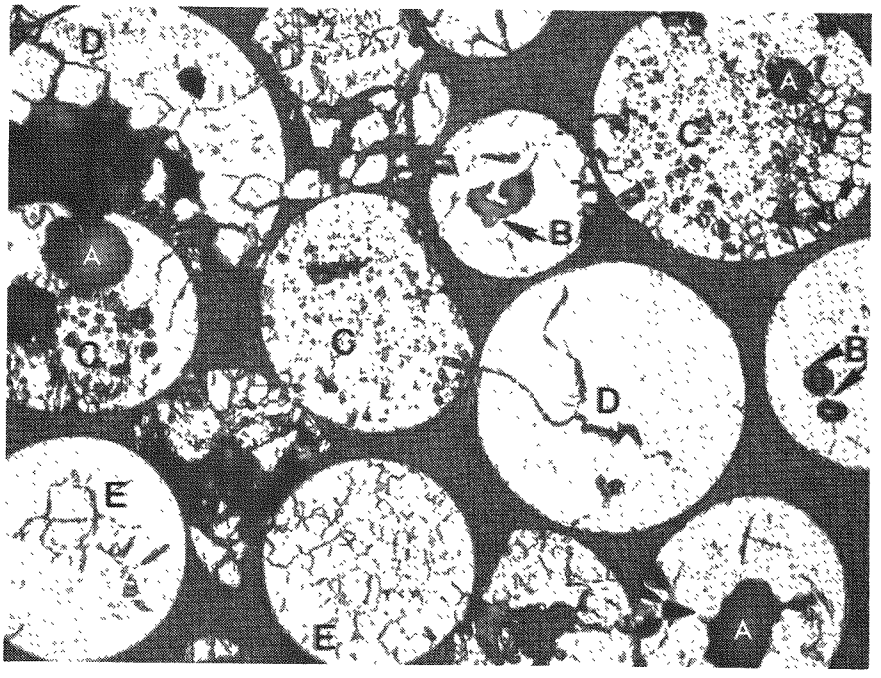

FIGURE 21 - Cross section of a sample of microspheres taken from the microsphere-fueled LRHS capsule. (220X)

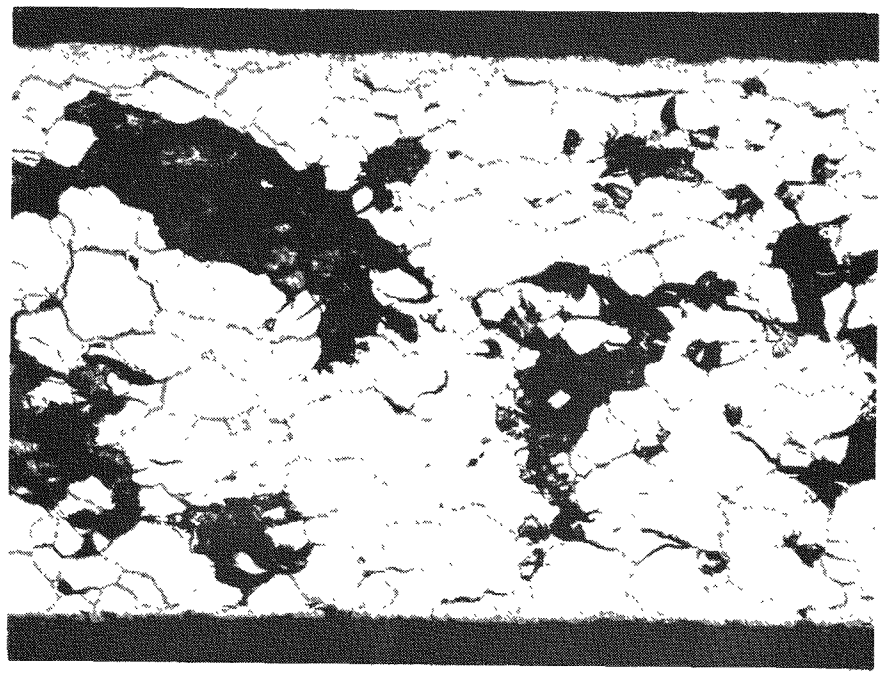

FIGURE 22 - Photomicrograph of the inner liner. (110X)

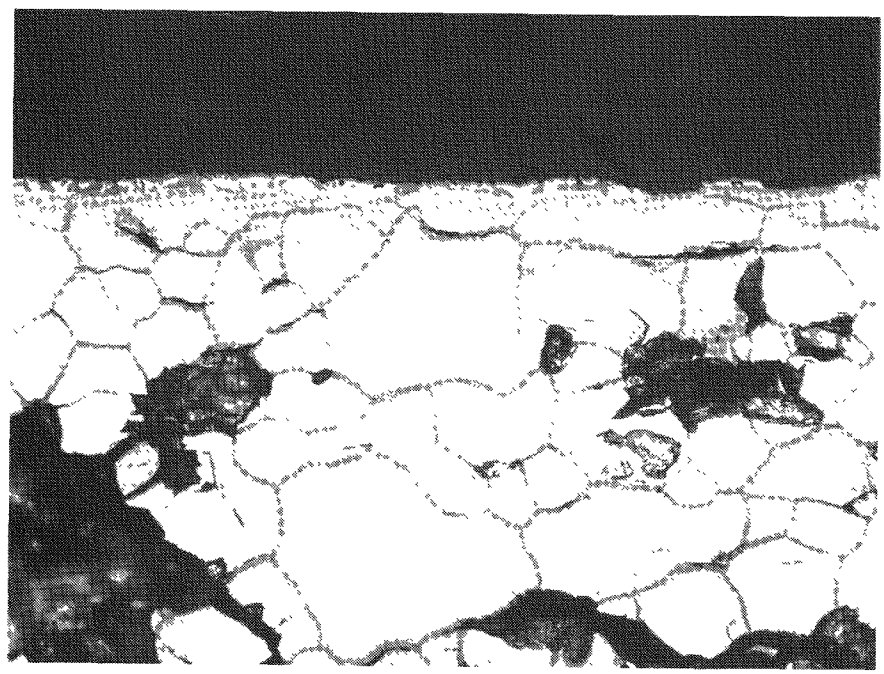

FIGURE 23 - Photomicrograph of the outside edge of the inner liner showing the fuel-liner reaction zone. (220X)

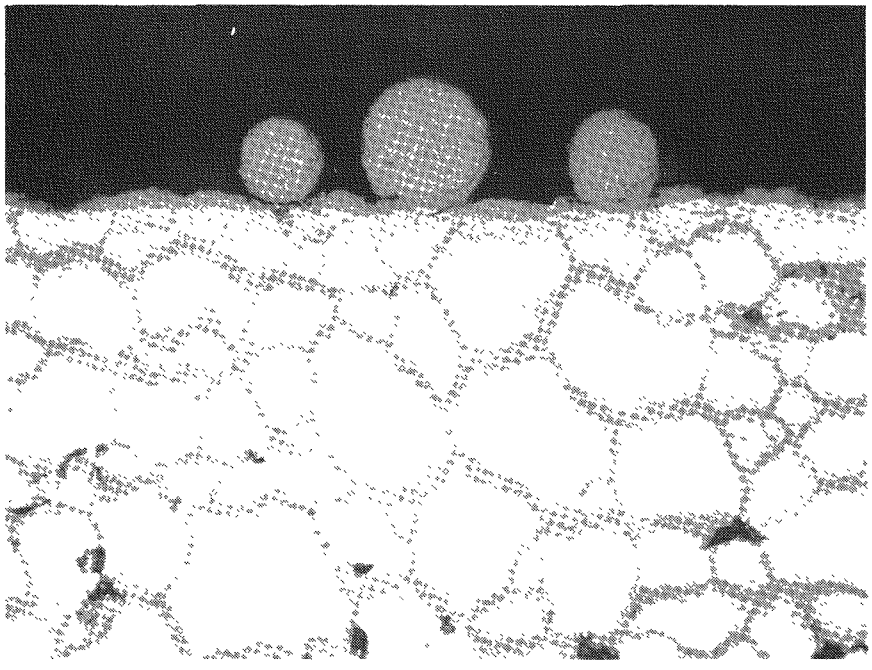

FIGURE 24 - Photomicrograph of outside edge of inner liner showing the relationship of retained microspheres with the liner surface. (220X)

Several microspheres can be seen adhering to the surface, and the reaction layer at the surface extends into the microspheres. While this sample was not microprobed, experience suggests that it contains plutonium, tantalum, and oxygen and is probably $PuO_2 \cdot 2Ta_2O_5$. The grain boundaries show a decrease in tungsten. Although no x-ray diffraction studies were done, prior experience has shown the intergranular material to be Ta_2O_5.

Inside Edge of Inner Liner A photomicrograph of the inside edge of the inner liner is shown in Figure 25. In general this interface is not much different from the outside edge of the liner, which is the fuel-inner liner interface (refer to schematic in Figure 4). The major difference is in the absence of the white impurity-bearing layer. In the gray layer, at the edge of the sample, electron microprobe analysis revealed tantalum, tungsten, oxygen, and aluminum, with no chromium, iron, silicon, cobalt, nickel, or plutonium. No tungsten was found in the gray layer, although a concentration was found on the outside edge of the gray layer. No explanation for this concentration can be given. The origin of the aluminum is unknown although it probably came from minute particles of polishing compound which became trapped in the porous reaction layer.

A microhardness traverse across the inner liner is shown in Figure 26. Care was taken to obtain hardness values in the centers of individual grains because the brittleness of the grain boundaries rendered measure-

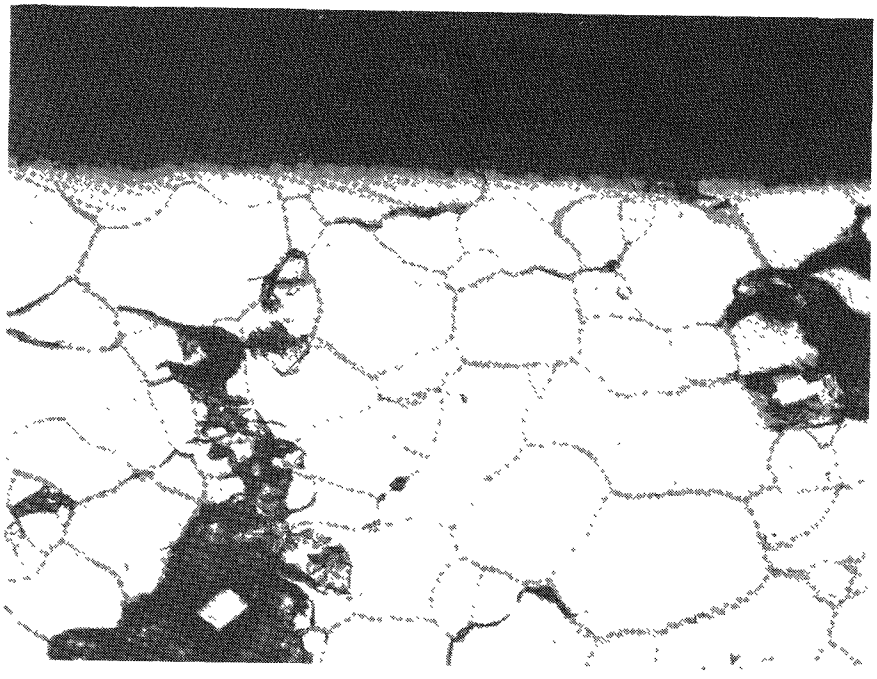

FIGURE 25 - Photomicrograph of the inside edge of the inner liner. (220X)

ments near the boundaries impossible. The high hardness values verify the brittleness of the material. Some of the indentations produced cracks which give false hardness readings and further testify to the brittleness of the alloy.

Fuel-Outer Liner Interface Two different microstructures were found in the outer liner. A photomicrograph of the first type of the fuel-outer liner interface is shown in Figure 27. The white reaction product at the edge is similar to that shown in Figure 23. Electron microprobe analysis of this layer revealed the presence of chromium, iron, nickel, and plutonium, with a small amount of silicon. Tantalum and tungsten were depleted along the edge although they were still present. The grain boundary penetration of oxide is appreciably less than in the case of the inner liner. Presumably this is because of the lower operating temperature of the outer liner compared to the inner liner.

The second type of microstructure from the same sample is shown in Figure 28. This anomalous structure was very difficult to resolve and etching failed to reveal the structure. Electron microprobe analysis revealed the presence of chromium, iron, cobalt, nickel, silicon, plutonium, oxygen, and aluminum. Tantalum and tungsten were present although depleted from their original concentration.

Microhardness traverses were made across the two areas, and these are shown in Figure 29. The traverses are virtually identical. With the

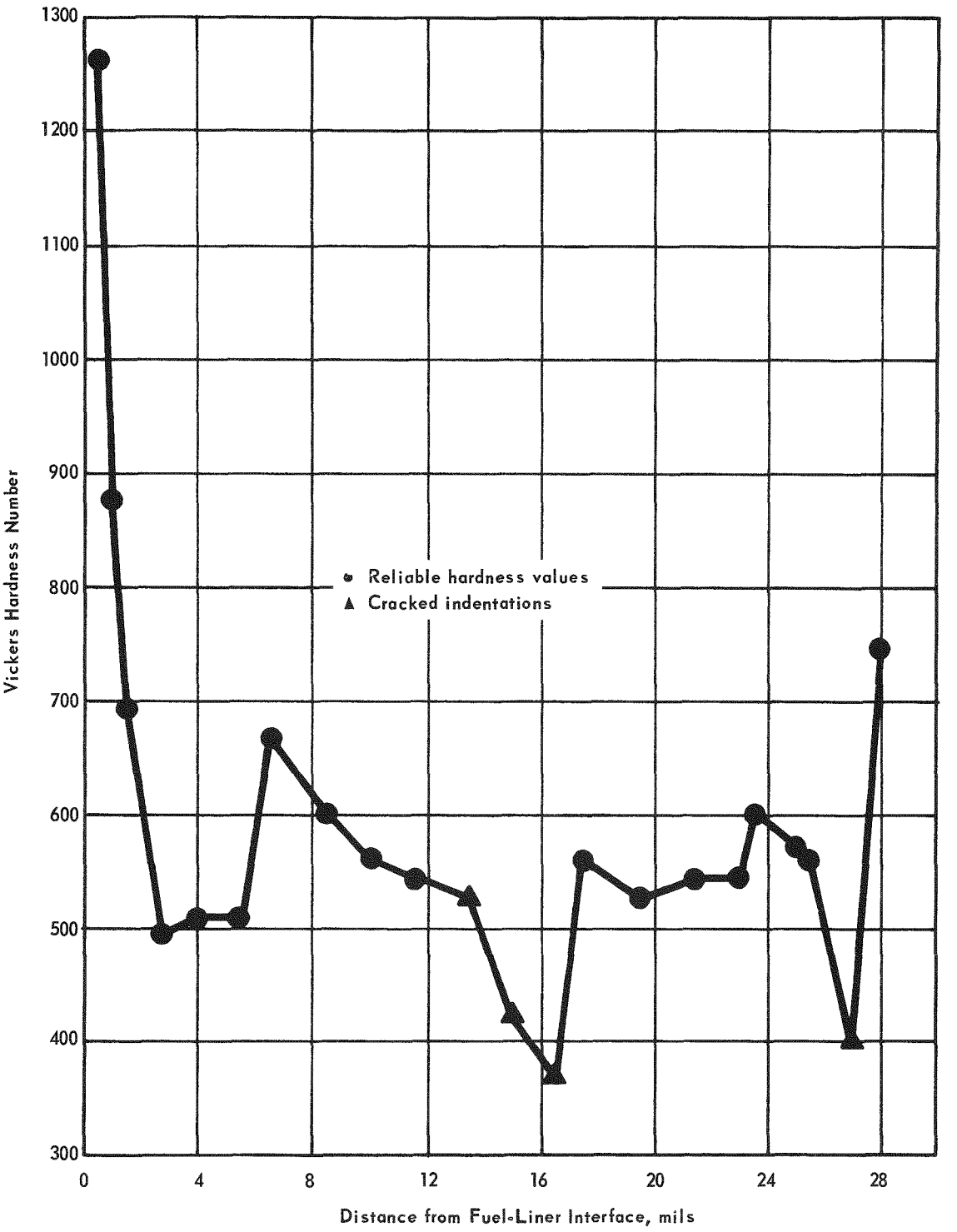

FIGURE 26 - Microhardness traverse across the inner liner.

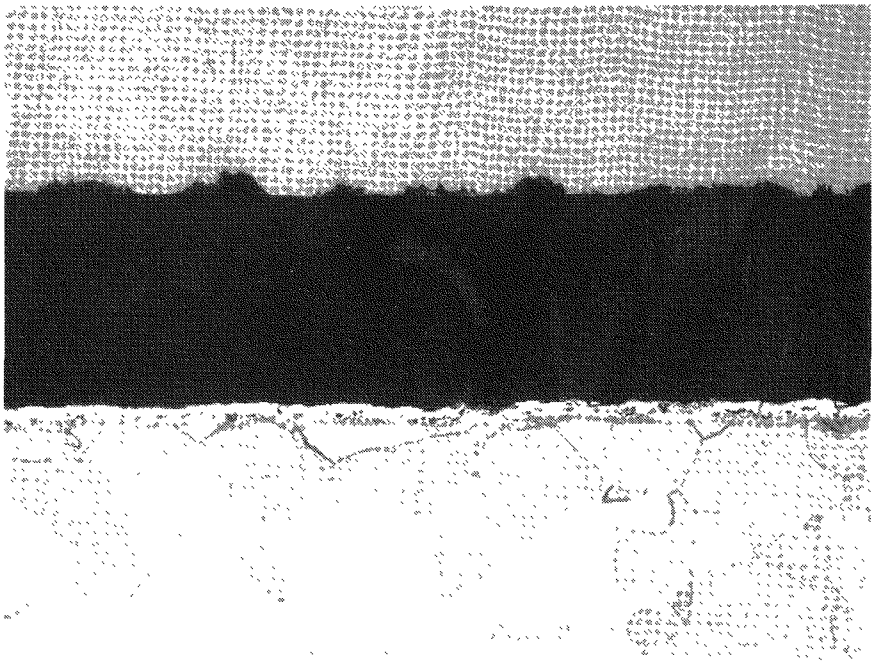

FIGURE 27 - Photomicrograph of the normal structure of the inside edge of the outside liner. (220X)

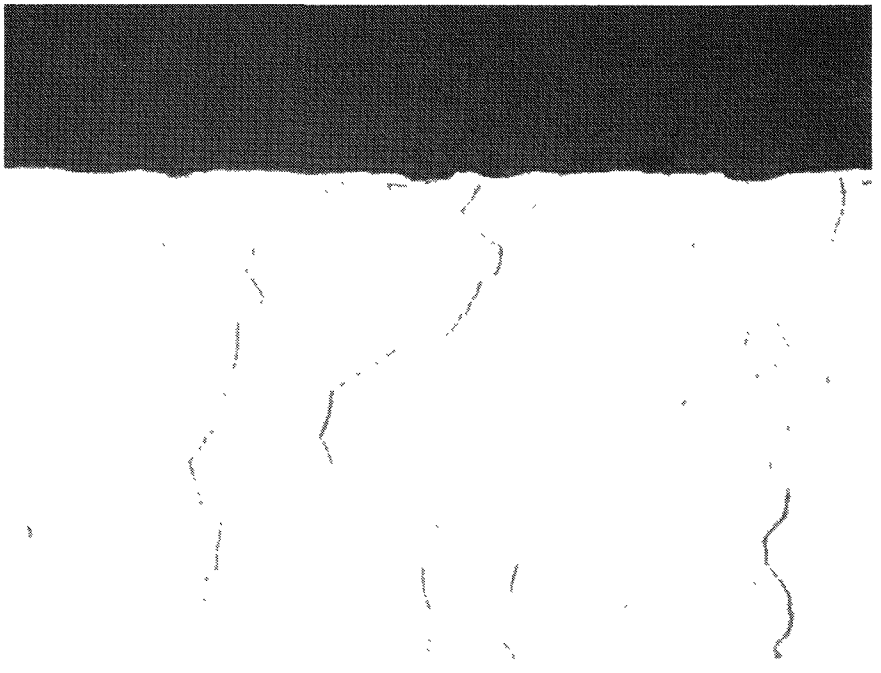

FIGURE 28 - Photomicrograph of the anomalous microstructure from the inside edge of the outside liner. (220X)

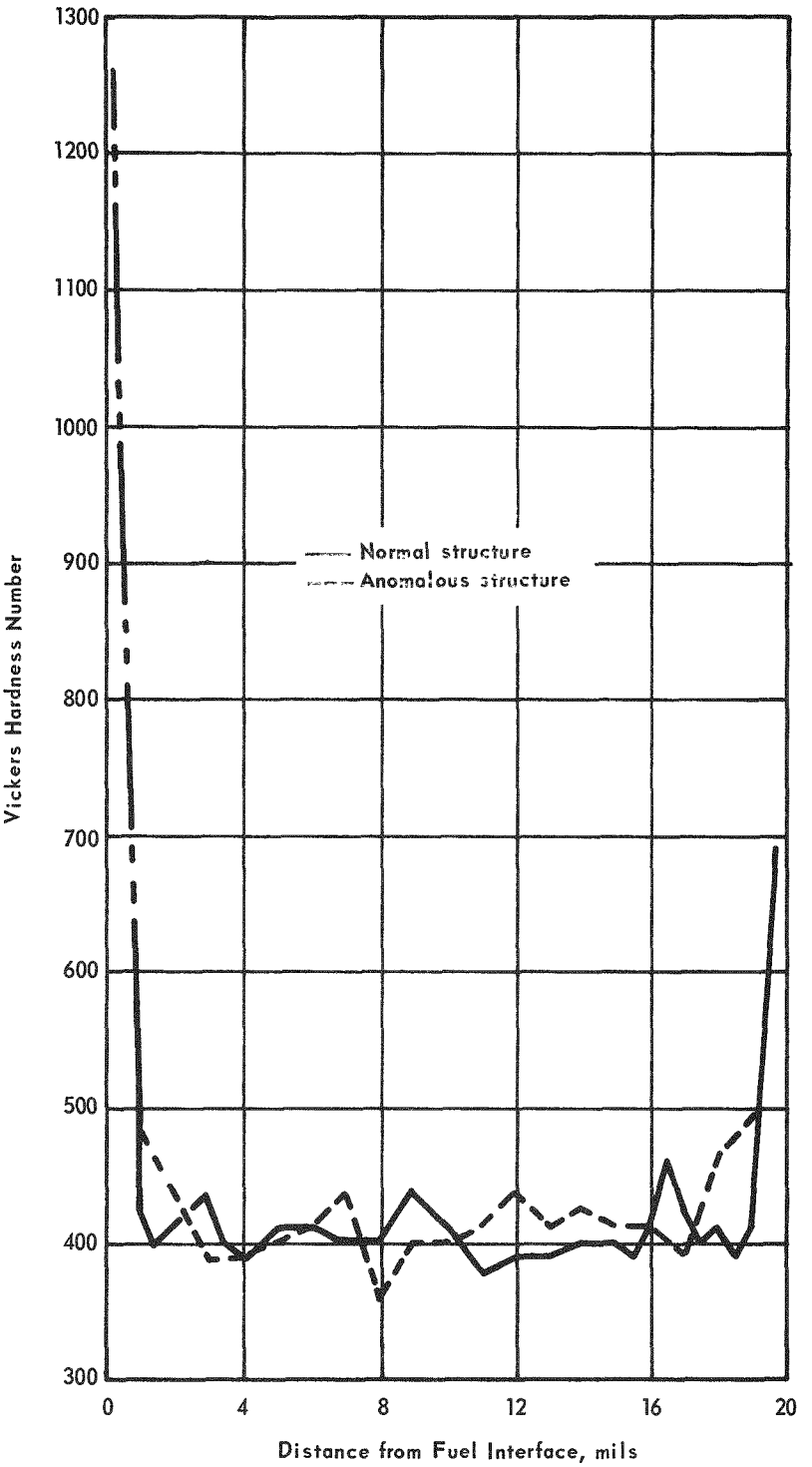

FIGURE 29 - Microhardness traverse across the outside liner at the normal structure and the anomalous structure.

exception of the presence of aluminum, oxygen, and cobalt in the anomalous structure, the two areas are identical in all respects. Oxygen in interstitial solid solution is the most likely cause of the difference, although no explanation can be offered at this time for the variations in oxygen content. The differences in structure are real and numerous attempts were made to bring out the anomalous structure.

Outer Liner-Strength Member Interface Photomicrographs of the outside edge of the outside liner are shown in Figures 30 and 31. These photomicrographs show the normal and anomalous microstructure discussed previously. The microprobe results on both of these areas were virtually identical. A decrease in tantalum was found near the surface along with an increase in tungsten. The samples were checked for oxygen, chromium, aluminum, iron, silicon, cobalt, nickel, and plutonium, but none was found except in the case of the normal microstructure where some oxygen was found near the interface. The reason for the depletion of tantalum is unknown, although oxidation may have occurred on the surface and the reaction product was lost during the metallographic preparation.

Strength Member A photomicrograph of a crack in the strength member is given in Figure 32. This figure shows the intergranular nature of the crack. Microhardness data for this sample are given in Figure 33. It is obvious that the alloy is extremely hard indicating the absorption of considerable oxygen.

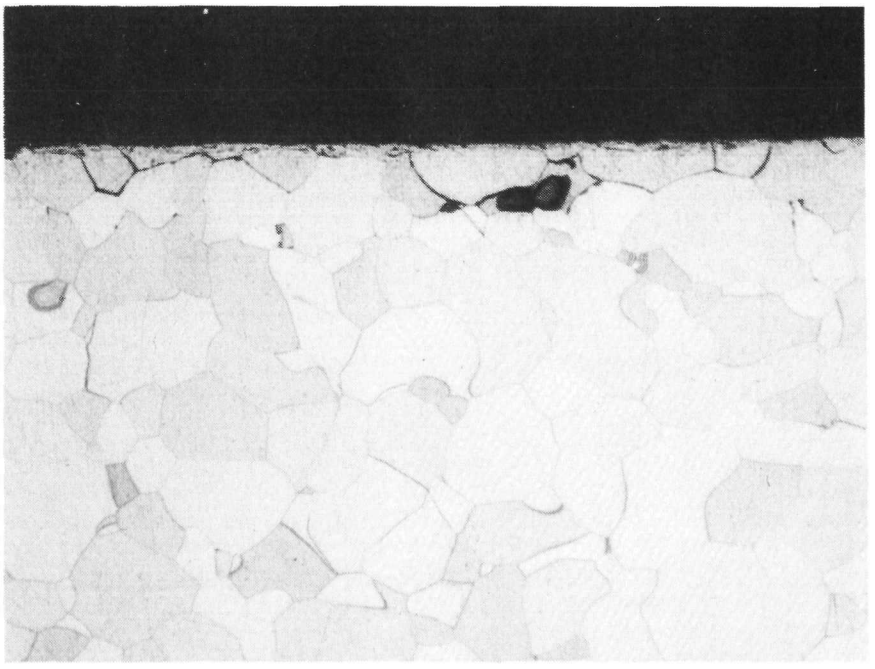

FIGURE 30 - Photomicrograph of the outside edge of the outer liner; normal structure. (220X)

FIGURE 31 - Photomicrograph of the outside edge of the outer liner; anomalous structure. (220X)

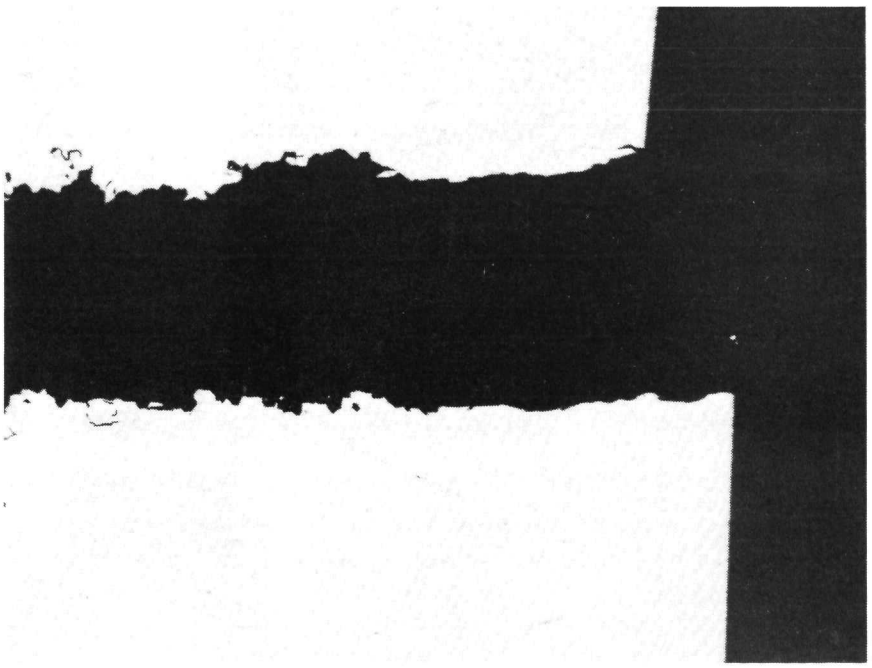

FIGURE 32 - Cross section of crack in strength member showing intergranular nature of the crack. (unetched, 54X)

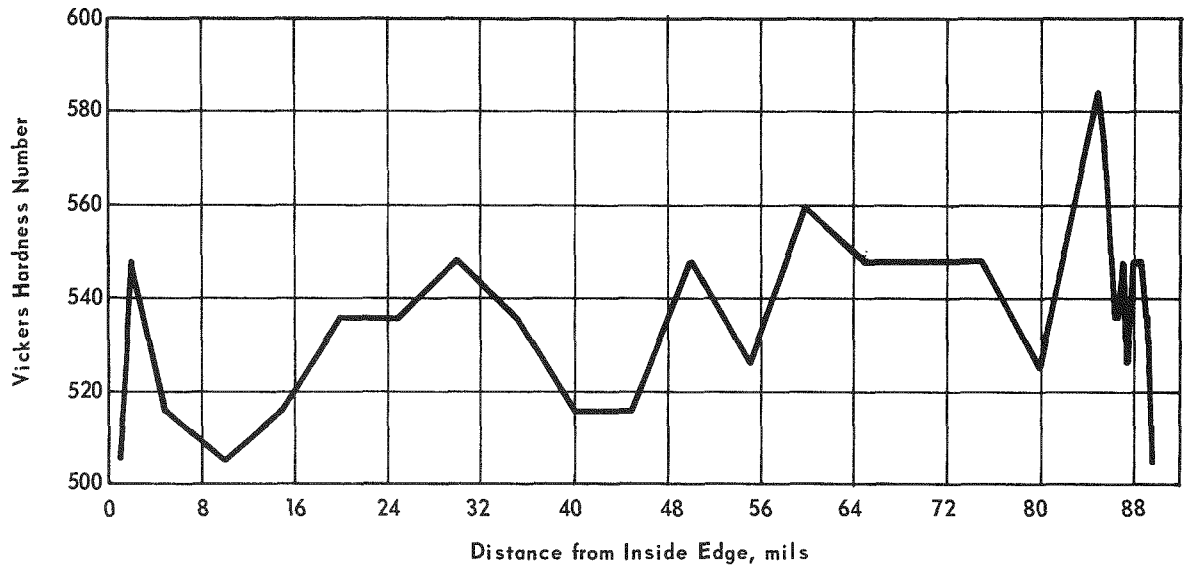

FIGURE 33 - Microhardness traverse across strength member.

Strength Member-Coating Interface A photomicrograph of the outside edge of the strength member showing the Al_2O_3 coating is shown in Figure 34. Microprobe analysis was made along the line indicated and the analysis of each zone is as follows:

Zone A: O, Al, Fe, Si, Co, Ni, Hf, Ta
Zone B: O, Al, Hf, Ta
Zone C: Ta, W
Zone D: O, Hf, Ta, W.

The tungsten content in Zone C was quite high, while the tantalum content was low, and in the region adjacent to Zone B was essentially zero. The iron, silicon, cobalt, and nickel appeared only at the outside edge of Zone A. The origin of these elements is unknown.

Weld Sections Cross sections of each weld were taken as an aid to the Fabrication Group to determine the efficiency of their operation. Other than to determine the depth of penetration and amount of porosity, if any, no attempt has been made to examine these welds in detail. Photomicrographs of the welds are given in Figures 35 through 39. The exact location of each weld can be determined from Figure 20.

Oxygen Analyses Oxygen analyses on samples taken from the microsphere fueled capsule were also performed and these are summarized in Table 10.

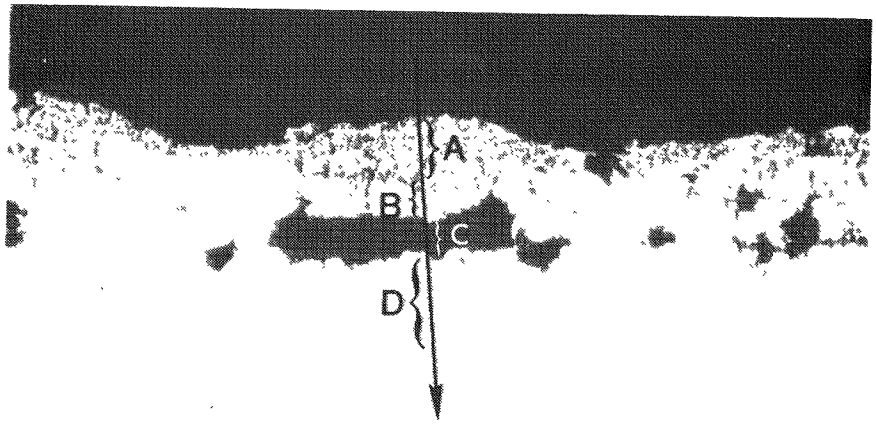

FIGURE 34 - Photomicrograph of the outside edge of the strength member showing the Al_2O_3 spray coating. (unetched, 220X)

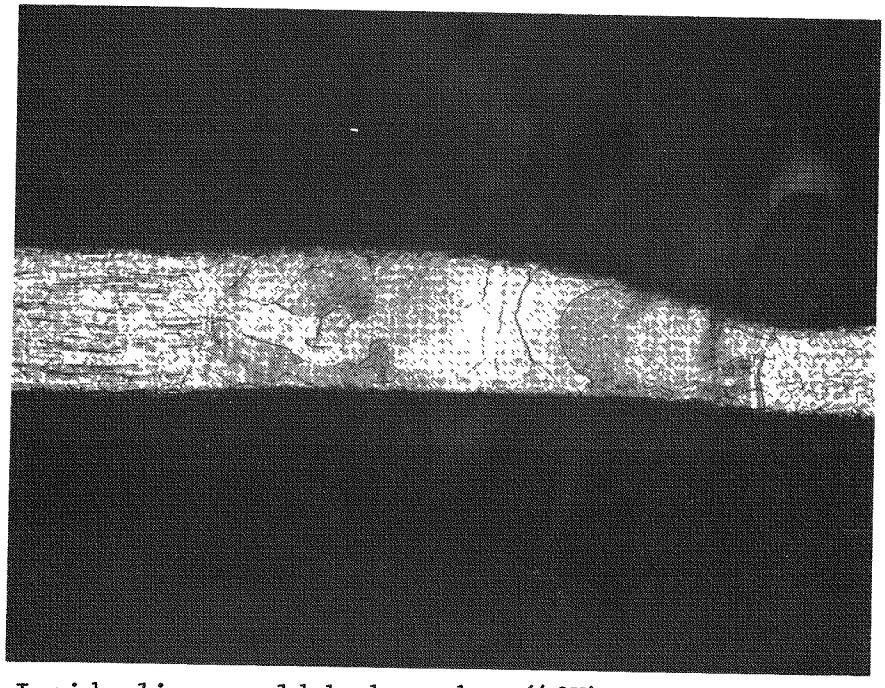

FIGURE 35 - Inside liner weld, body end. (40X)

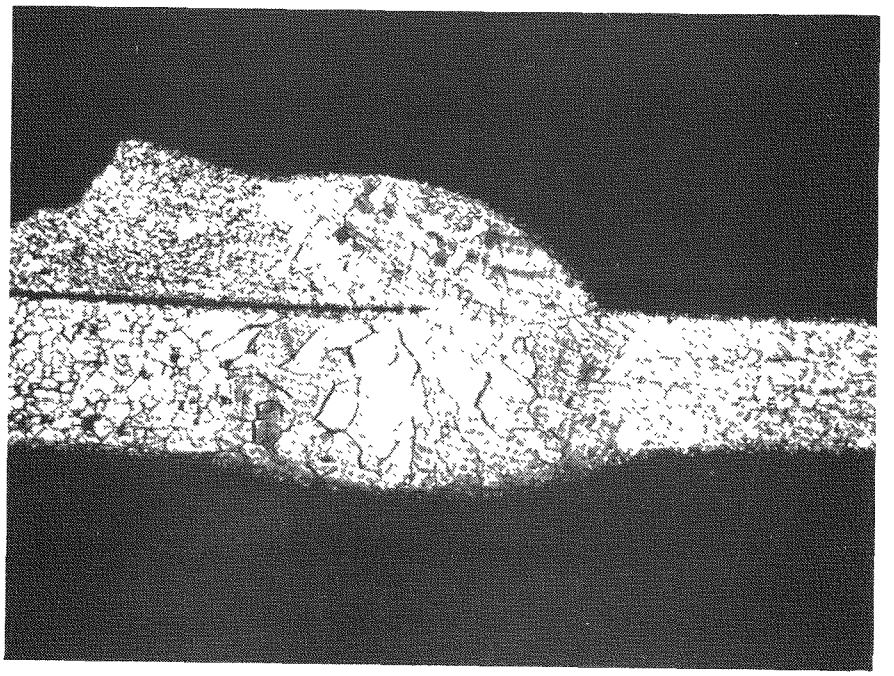

FIGURE 36 - Inside liner weld and fuel closure ring weld. (40X)

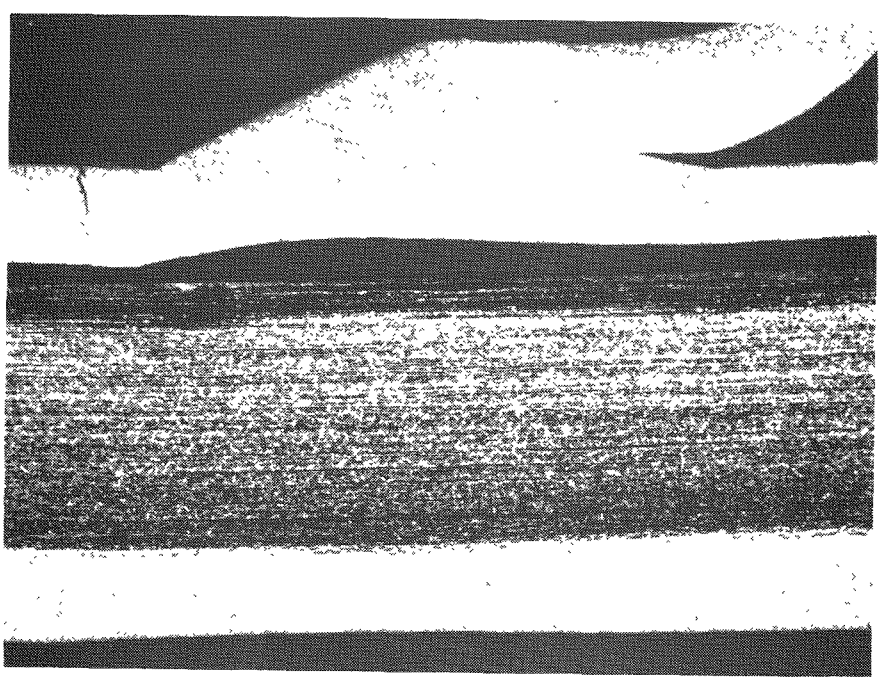

FIGURE 37 - Outside liner weld, body end and strength member. (20X)

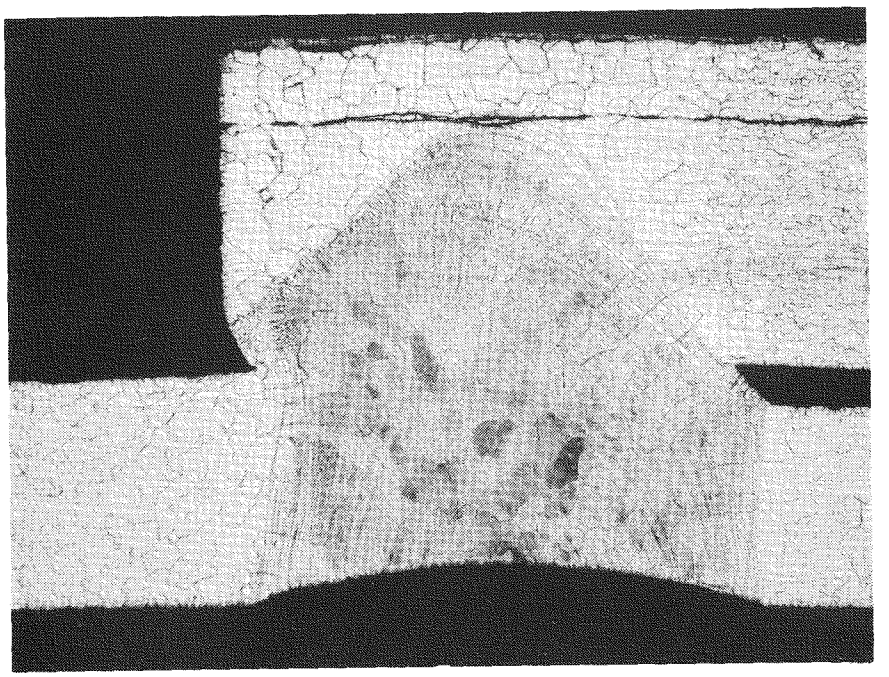

FIGURE 38 - Outside liner weld, cap end. (62X)

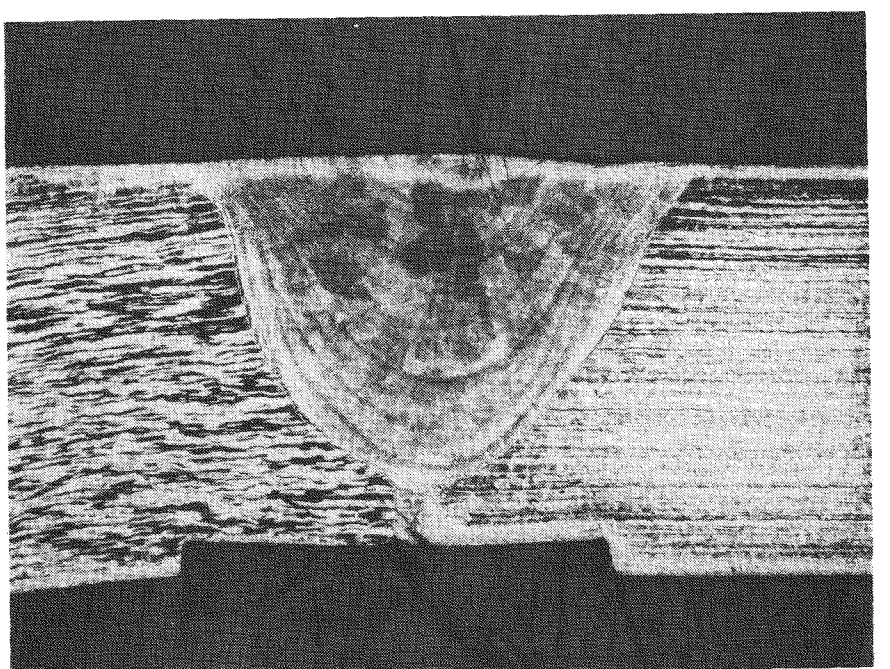

FIGURE 39 - Strength member weld, 86.5% penetration. (25X)

Comparison of these data with those in Table 8 shows that the oxygen uptake is much more serious in this capsule than in the cermet fueled capsule. Several reasons may be advanced for this. Among these are:

1. The stoichiometry of the cermet fuel form is less than the microsphere fuel form, resulting in a fuel more stable to tantalum alloys.

2. There is a greater quantity of tantalum in the cermet-fueled capsule so that more oxygen can be absorbed as the system equilibrates.

3. The cermet fuel form had a molybdenum and ThO_2 overcoat which probably acted as a diffusion barrier.

Each of the possibilities probably contributed some effect although the actual contribution of each is unknown.

Table 10

SUMMARY OF OXYGEN ANALYSES OF SAMPLES TAKEN FROM THE MICROSPHERE FUELED LRHS

Sample	Oxygen Content (ppm)
Spacer	796
Inner Liner (middle of source)	>10,000
Inner Liner (1 in. from dome)	7,054
Outer Liner (1 in. from dome)	2,117
Strength Member (middle of source)	4,250
Strength Member (1 in. from dome)	>10,000
Strength Member (middle of source-oxide removed)	4,472

CONCLUSIONS

1. The T-111 strength member of the microsphere-fueled capsule was found to be cracked upon removal from the clad.

2. Considerable grain boundary oxidation of the Ta-10%W liner of the microsphere capsule occurred.

3. Considerable reaction between the fuel impurities and the Ta-10%W liner occurred in the microsphere fueled capsule.

4. The Ta-10%W liner and the T-111 strength member from the Mo-cermet fueled capsule were not embrittled.

5. The Al_2O_3 spray coating reacted with the T-111 strength member causing

considerable hardness increase at the outside edge due to oxygen absorption.

6. The Al_2O_3 spray coating appeared to react with the Pt-20%Rh clad.

7. Considerable grain growth of the Pt-20%Rh clad occurred.

8. Some swelling of the cermet fuel occurred.

9. Approximately 81.3% of the helium generated was released at the operating temperature of the capsule.

10. All welds examined appeared to be sound, with no porosity.

ACKNOWLEDGMENTS

The authors would like to thank Mr. P. E. Teaney for his assistance in defueling the capsules, Mr. D. L. Roesch for electron microprobe analyses, Mr. R. E. Zielinski for the use of some of the helium retention data, Mr. J. Y. Jarvis for the oxygen analyses, and Mr. R. E. Fitzharris for his assistance in the technical editing of this report.

REFERENCES

1. Battelle Memorial Institute, private communication.

2. Mound Laboratory Isotopic Power Fuels Programs: October-December 1970, MLM-1791 (February 18, 1971) pp. 32-33.

3. W. M. Pardue - private communication.

APPENDIX A

SUMMARY OF DATA ON ANNULAR FUEL RINGS[a]

Specimen	Dimensions						Power (W)	Thermal Density (W/cc)
	As Machined			After Coating				
	OD (in.)	ID (in.)	Thickness (in.)	OD (in.)	ID (in.)	Thickness (in.)		
AA65	1.352	0.603	0.397	1.364	0.587	0.407	24.49	3.08
AA66	1.352	0.604	0.437	1.363	0.589	0.450	27.38	3.12
AA67	1.354	0.560	0.481	1.366	0.592	0.490	30.45	3.19
AA69	1.352	0.614	0.541	1.363	0.598	0.553	33.78	3.16
AA70	1.346	0.601	0.520	1.362	0.580	0.538	29.73	2.83
AA71	1.347	0.601	0.481	1.361	0.575	0.505	29.18	2.95
AA72	1.352	0.602	0.496	1.364	0.591	0.510	31.05	3.13
Average	1.351	0.598	0.479	1.366	0.587	0.490	29.43	3.07

[a] Reference 1.

APPENDIX B

HELIUM RELEASE MEASUREMENTS

The amount of helium in the system was determined as follows:

1. The internal volume of the capsule

   $= \frac{\pi d^2}{4} \times \ell = \frac{\pi}{4} \times 1.380^2 \times 5.314$

   $= 7.946 \text{ in.}^3$

2. The fuel volume is calculated to be (from Table 1) 4.101 in.^3

3. The volume of the spacers is calculated to be 2.345 in.^3

4. Therefore the free volume of the capsule is

   $7.946 - 4.101 - 2.345 = 1.500 \text{ in.}^3$
   $= 24.580 \text{ cm}^3$

5. The composition of the gas removed from the system was

He	88.2
Ar	9.4
N_2	1.7
O_2	0.5
H_2O	0.1
	99.9%

   Since the welding box atmosphere was argon, the ratio of the He to Ar can be used to determine the volume of helium

   $\frac{V_{He}}{24.58} = \frac{88.2}{9.4}$

   $V_{He} = 230.6 \text{ cc}$

6. Since there were 515 g of fuel in the capsule

   $\frac{230.6}{515} = 0.4478 \text{ cc/g}$ of fuel was released during the test

7. The theoretical amount of helium generated in the fuel was calculated to be 0.5504 cc/g after 9100 hr.

8. Therefore the percent of helium released was

$$\frac{0.4478}{0.5504} = 81.3\%$$

9. Measurements of helium released during high temperature heating yielded 0.0871 cc/g or 15.8% of theoretical

10. Thus a total of 97.1% of the helium has been accounted for.

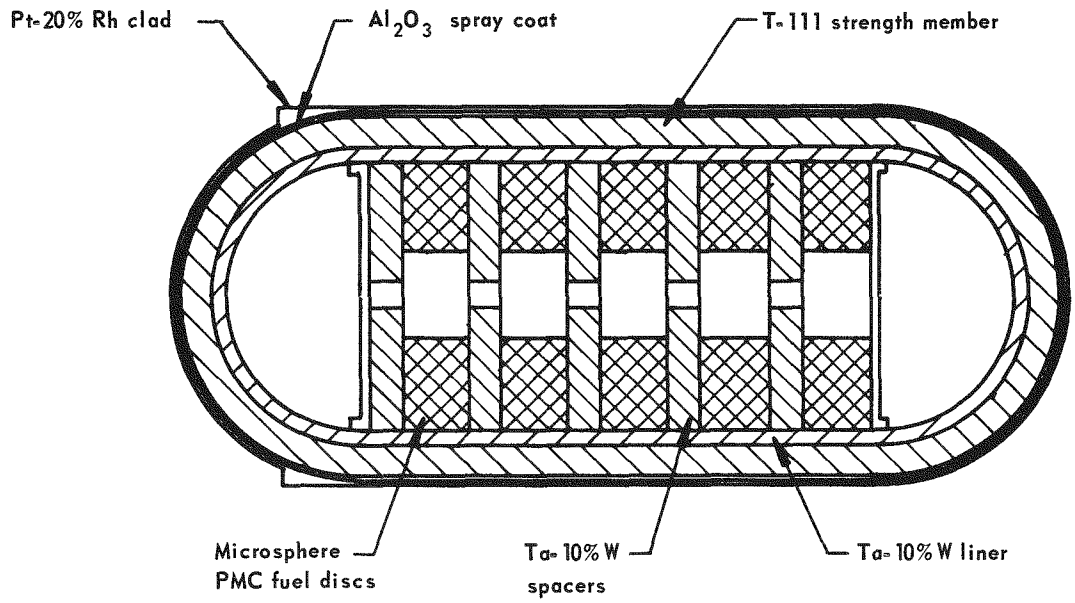

FIGURE C-1 - Microsphere-cermet fueled capsule.

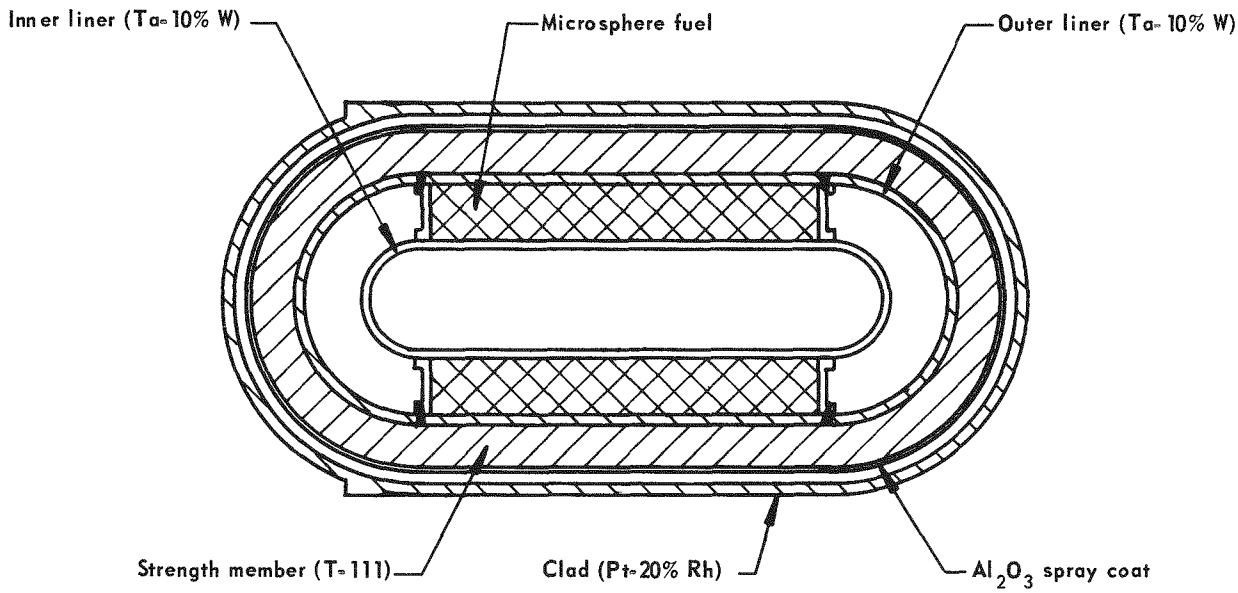

FIGURE C-2 - Microsphere fueled capsule

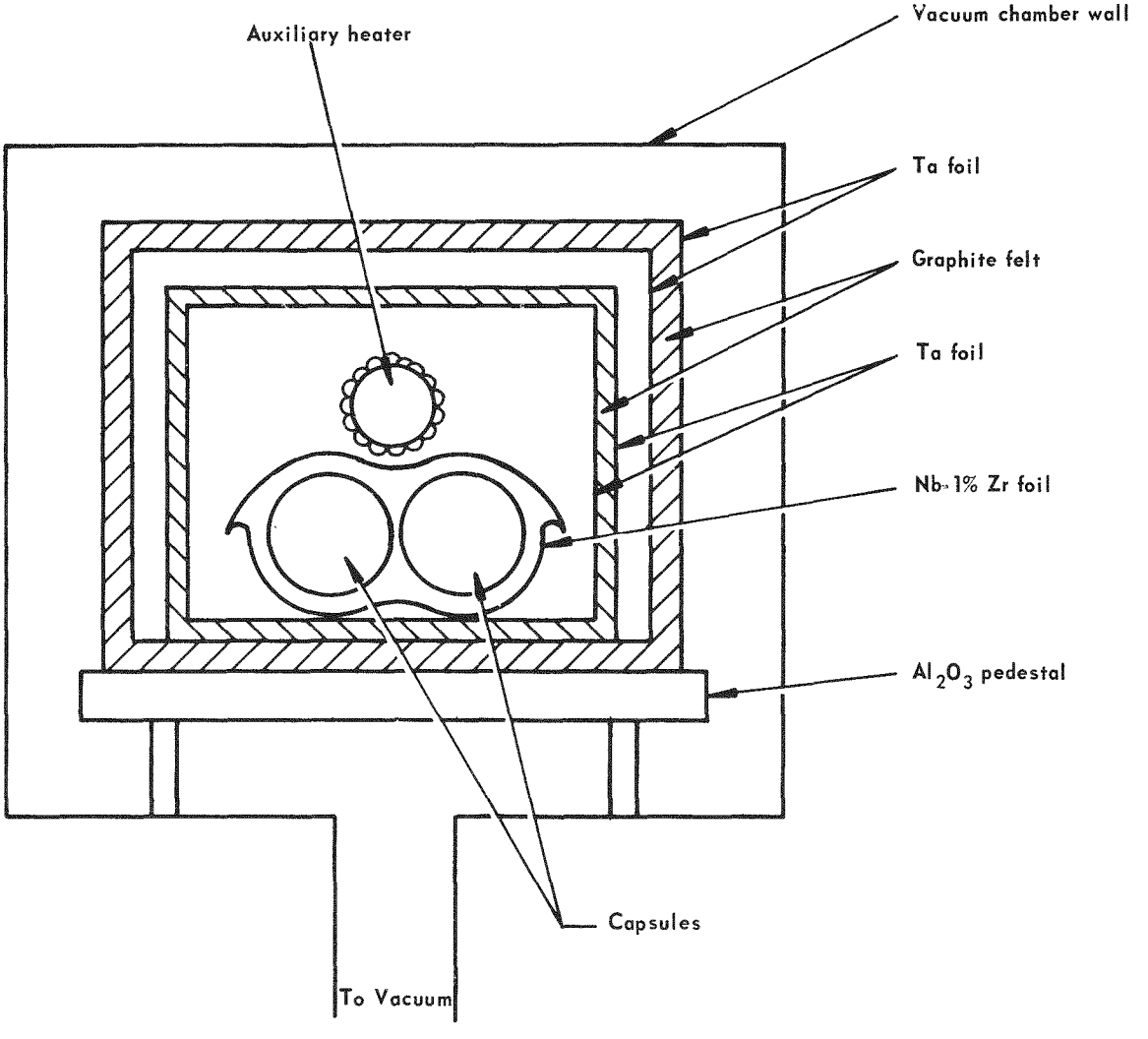

FIGURE C-3 - Test configuration